

This is an Open Access document downloaded from ORCA, Cardiff University's institutional repository: <https://orca.cardiff.ac.uk/id/eprint/109925/>

This is the author's version of a work that was submitted to / accepted for publication.

Citation for final published version:

Barrientos, Natalia, Lear, Caroline , Jakobsson, Martin, Stranne, Christian, O'Regan, Matt, Cronin, Thomas M., Gukov, Alexandr Y. and Coxall, Helen K. 2018. Arctic Ocean benthic foraminifera Mg/Ca ratios and global Mg/Ca-temperature calibrations: New constraints at low temperatures. *Geochimica et Cosmochimica Acta* 236 , pp. 240-259. 10.1016/j.gca.2018.02.036

Publishers page: <http://dx.doi.org/10.1016/j.gca.2018.02.036>

Please note:

Changes made as a result of publishing processes such as copy-editing, formatting and page numbers may not be reflected in this version. For the definitive version of this publication, please refer to the published source. You are advised to consult the publisher's version if you wish to cite this paper.

This version is being made available in accordance with publisher policies. See <http://orca.cf.ac.uk/policies.html> for usage policies. Copyright and moral rights for publications made available in ORCA are retained by the copyright holders.





Arctic Ocean benthic foraminifera Mg/Ca ratios and global Mg/Ca-temperature calibrations: New constraints at low temperatures

Natalia Barrientos^{a,b,*}, Caroline H. Lear^c, Martin Jakobsson^{a,b}, Christian Stranne^{a,b},
Matt O'Regan^{a,b}, Thomas M. Cronin^d, Alexandr Y. Gukov^e, Helen K. Coxall^{a,b}

^a Department of Geological Sciences, Stockholm University, Stockholm 10691, Sweden

^b Bolin Centre for Climate Research, Stockholm University, Stockholm 10691, Sweden

^c School of Earth and Ocean Sciences, Cardiff University, Main Building, Park Place, Cardiff CF10 3AT, UK

^d U.S. Geological Survey, Reston, VA, USA

^e Lena Delta Reserve, Akademika Fedorova Str. 28, 678400 Tiksi, Yakutia, Russia

Received 1 June 2017; accepted in revised form 22 February 2018; available online xxxx

Abstract

We explore the use of Mg/Ca ratios in six Arctic Ocean benthic foraminifera species as bottom water palaeothermometers and expand published Mg/Ca-temperature calibrations to the coldest bottom temperatures (<1 °C). Foraminifera were analyzed in surface sediments at 27 sites in the Chukchi Sea, East Siberian Sea, Laptev Sea, Lomonosov Ridge and Petermann Fjord. The sites span water depths of 52–1157 m and bottom water temperatures (BWT) of –1.8 to +0.9 °C. Benthic foraminifera were alive at time of collection, determined from Rose Bengal (RB) staining. Three infaunal and three epifaunal species were abundant enough for Mg/Ca analysis. As predicted by theory and empirical evidence, cold water Arctic Ocean benthic species produce low Mg/Ca ratios, the exception being the porcelaneous species *Quinqueloculina arctica*. Our new data provide important constraints at the cold end (<1 °C) when added to existing global datasets. The refined calibrations based on the new and published global data appear best supported for the infaunal species *Nonionella labradorica* (Mg/Ca = $1.325 \pm 0.01 \times e^{(0.065 \pm 0.01 \times \text{BWT})}$, $r^2 = 0.9$), *Cassidulina neoteretis* (Mg/Ca = $1.009 \pm 0.02 \times e^{(0.042 \pm 0.01 \times \text{BWT})}$, $r^2 = 0.6$) and *Elphidium clavatum* (Mg/Ca = $0.816 \pm 0.06 + 0.125 \pm 0.05 \times \text{BWT}$, $r^2 = 0.4$). The latter is based on the new Arctic data only. This suggests that Arctic Ocean infaunal taxa are suitable for capturing at least relative and probably semi-quantitative past changes in BWT. Arctic *Oridorsalis tener* Mg/Ca data are combined with existing *O. umbonatus* Mg/Ca data from well saturated core-tops from other regions to produce a temperature calibration with minimal influence of bottom water carbonate saturation state (Mg/Ca = $1.317 \pm 0.03 \times e^{(0.102 \pm 0.01 \times \text{BWT})}$, $r^2 = 0.7$). The same approach for *Cibicidoides wuellerstorfi* yields Mg/Ca = $1.043 \pm 0.03 \times e^{(0.118 \pm 0.1 \times \text{BWT})}$, $r^2 = 0.4$. Mg/Ca ratios of the porcelaneous epifaunal species *Q. arctica* show a clear positive relationship between Mg/Ca and $\Delta[\text{CO}_3^{2-}]$ indicating that this species is not suitable for Mg/Ca-palaeothermometry at low temperatures, but may be useful in reconstructing carbonate system parameters through time.

© 2018 The Authors. Published by Elsevier Ltd. This is an open access article under the CC BY-NC-ND license (<http://creativecommons.org/licenses/by-nc-nd/4.0/>).

Keywords: Benthic foraminifera; Mg/Ca temperature calibration; Arctic Ocean; Core-tops

* Corresponding author at: Department of Geological Sciences, Stockholm University, Stockholm 10691, Sweden.
E-mail address: natalia.barrientos@geo.su.se (N. Barrientos).

<https://doi.org/10.1016/j.gca.2018.02.036>

0016-7037/© 2018 The Authors. Published by Elsevier Ltd.

This is an open access article under the CC BY-NC-ND license (<http://creativecommons.org/licenses/by-nc-nd/4.0/>).

1. INTRODUCTION

Instrumental records provide a short perspective on Arctic Ocean temperatures, revealing ongoing warming over recent decades (Quadfasel et al., 1991; Carmack et al., 1995; Schauer et al., 2004; Polyakov et al., 2005; Schauer et al., 2008; Polyakov et al., 2012). Quantifying long-term changes in Arctic Ocean temperatures using palaeoceanographic proxies is necessary to gain wider perspective on the magnitude of the recent changes and to help identify links between ocean-climate feedback processes (Serreze and Barry, 2011). Mg/Ca-palaeothermometry is a useful geochemical tool for reconstructing bottom water temperatures (BWT) in the geological past. Mg/Ca ratios have the advantage over $\delta^{18}\text{O}$ palaeothermometry in that they are independent of changes in seawater $\delta^{18}\text{O}$ that arise from ice growth and decay (Lear et al., 2000; Billups and Schrag, 2002; Martin et al., 2002). Mg and Ca are considered to have Myr long residence times in seawater (Broecker and Peng, 1992; Stanley and Hardie, 1999; Ries, 2010), thus Mg/Ca changes in marine calcite on Quaternary time scales should reflect ocean temperature rather than seawater Mg/Ca. The calculated benthic foraminiferal Mg/Ca-BWT relationship ('sensitivity') derived from existing calibrations is around $\sim 10 \pm 1\%$ or $\sim 0.1 \pm 0.01$ mmol/mol Mg/Ca increase per $^{\circ}\text{C}$ increase in ambient seawater temperature at calcification time (Rosenthal et al., 1997; Lear et al., 2002; Martin et al., 2002; Marchitto et al., 2007).

Existing benthic foraminifera Mg/Ca-palaeothermometry calibration studies span field BWT ranges of -1°C to 18°C (e.g. Rosenthal et al., 1997; Lear et al., 2002; Martin et al., 2002; Rathmann et al., 2004; Elderfield et al., 2006; Kristj nsd ttir et al., 2007; Marchitto et al., 2007; Healey et al., 2008; Yu and Elderfield, 2008; Elderfield et al., 2010; Lear et al., 2010; Skirbekk et al., 2016). While a few of the existing calibration studies include data from the cold end ($<1^{\circ}\text{C}$) of the global BWT spectrum (Rathburn and De Deckker, 1997; Martin et al., 2002; Rosenthal et al., 2006; Kristj nsd ttir et al., 2007; Yu and Elderfield, 2008; Lear et al., 2010; Quillmann et al., 2012; Skirbekk et al., 2016), these cannot be compared to the unique conditions occurring in the Arctic Ocean. Most available low temperature Mg/Ca data show extremely high Mg/Ca-BWT sensitivities with lower Mg/Ca values when compared to global calibrations. This has been linked to and conceptualized as the 'carbonate ion saturation ($\Delta[\text{CO}_3^{2-}]$) effect', i.e. that a threshold of $\Delta[\text{CO}_3^{2-}]$ exists below which Mg/Ca in foraminifera calcite decreases more as a consequence of a steep drop in bottom water $\Delta[\text{CO}_3^{2-}]$, and is less influenced by BWT (Martin et al., 2002; Elderfield et al., 2006; Marchitto et al., 2007; Yu and Elderfield, 2008). Quantification of this $\Delta[\text{CO}_3^{2-}]$ effect is challenging, since in reality bottom water $\Delta[\text{CO}_3^{2-}]$ is controlled not only by water depth and temperature but also by dissolved inorganic carbon (DIC) and alkalinity of bottom waters, which vary significantly between different ocean basins. The bottom waters bathing regions of Arctic Ocean seafloor sampled in this study, which includes the central Arctic and Russian Arctic shelves and slopes, all exhibit low temperatures (from -1.82 to 0.91°C

) and a relatively large range in bottom water $\Delta[\text{CO}_3^{2-}]$ (from -10.35 to 57.48 $\mu\text{mol/kg}$). This provides an opportunity to expand global calibrations at the coldest end of ocean waters and to explore whether a $\Delta[\text{CO}_3^{2-}]$ effect is controlling the Mg/Ca ratios in these cold waters. Some studies have suggested that salinity may also influence foraminiferal Mg/Ca (Dissard et al., 2010). However, the salinity ranges in our calibration sets are too small to fully evaluate this effect.

To date, while there has been success in using Mg/Ca in benthic ostracodes from the central Arctic Ocean (Farmer et al., 2011, 2012; Cronin et al., 2012), no equivalent data for benthic foraminifera exist. However, in Arctic sediments benthic foraminifera typically outnumber ostracodes, thus developing the proxy with foraminifera is considered worthwhile. The closest benthic foraminifera Mg/Ca data constraints, which are from the high latitude north Atlantic, show positive correlations between test Mg/Ca and temperature implying that benthic foraminifera Mg/Ca can faithfully record BWT in sub-Arctic and presumably Arctic environments (Kristj nsd ttir et al., 2007; Quillmann et al., 2012; Skirbekk et al., 2016). Field data from the Arctic Ocean are needed to validate the proxy given the unique and complex physical and chemical oceanic conditions prevailing there that may influence Mg/Ca partitioning into calcite.

Here we present the first investigation of benthic foraminifera Mg/Ca and BWT in the common Arctic Ocean species *Elphidium clavatum*, *Nonionella labradorica*, *Cassidulina neoteretis*, *Quinqueloculina arctica*, *Oridorsalis tener* and *Cibicides wuellerstorfi*. We also investigate the Mg/Ca relationships between bottom water $\Delta[\text{CO}_3^{2-}]$. The new cold-end constraints are incorporated into existing Mg/Ca compilations spanning broad BWT ranges from globally distributed sites. We conclude with a set of refined Mg/Ca-BWT calibrations appropriate for cold waters for five of the six species analyzed. The new calibrations provide important constraints for strengthening published temperature calibrations at the coldest extreme of ocean water temperatures.

1.1. The Arctic Ocean water masses

The vertical temperature structure of the Arctic Ocean is quite unlike other oceans. It has an inverted temperature profile with a strong halocline from the surface to 200 m reflecting the role of salinity, rather than temperature in driving Arctic Ocean stratification. The halocline comprises the coldest water mass layer (from -2 to 0°C) and its uppermost 50 m include the 'polar mixed layer' that is the freshest layer, derived from seasonal sea ice melt, fluvial inputs and Bering Strait inflow (Steele and Boyd, 1998). Below the halocline (~ 200 to 900 m water depth) sits the Atlantic water that is slightly warmer (0 – 2°C) and saltier than subsurface waters, derived largely from Atlantic inflow (Rudels et al., 1994; Rudels et al., 2012) (Fig. 1). Beneath ~ 900 m the Arctic Ocean is filled with Arctic deep water, which has more homogeneous thermal and salinity properties. The Chukchi Sea, from which several of our new core-top samples are retrieved, has its own unique characteristics

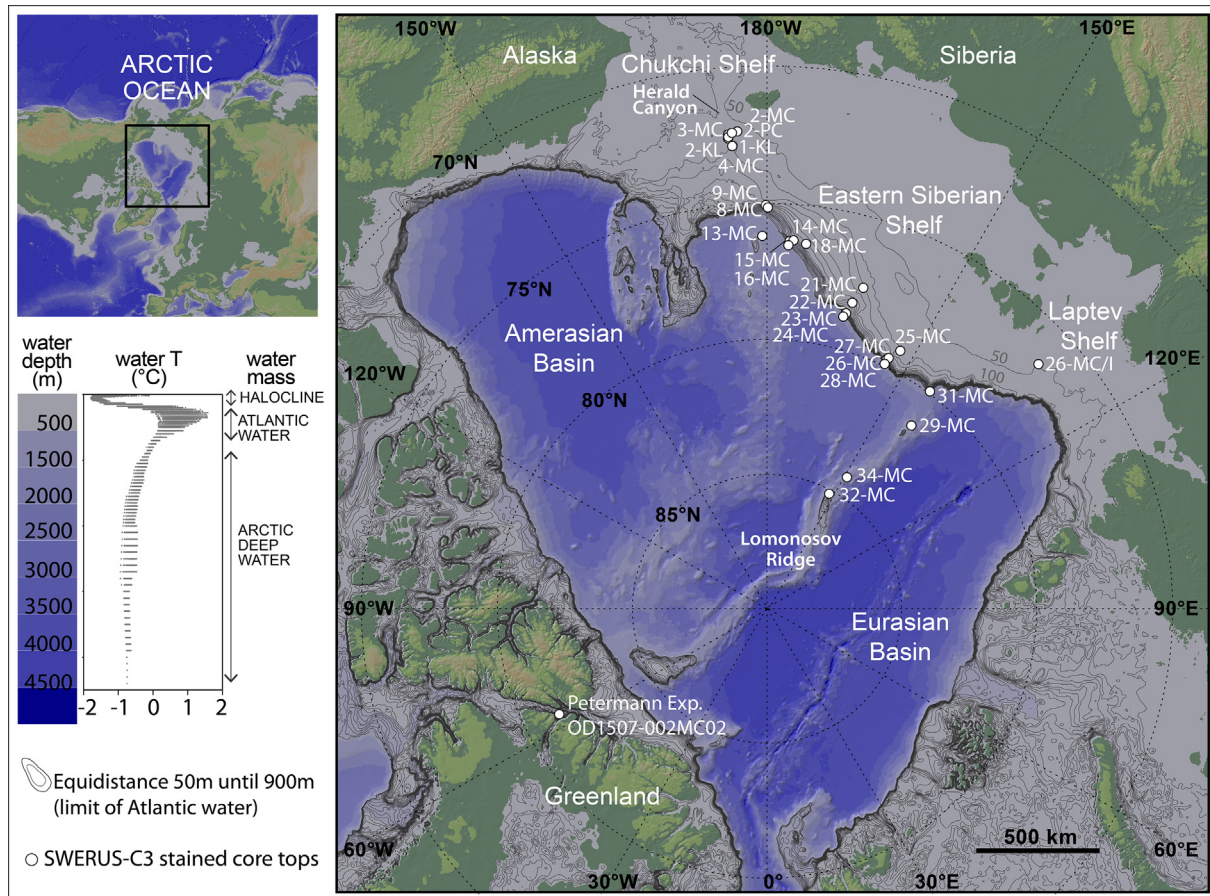


Fig. 1. Location of the 27 Arctic Ocean study sites used to build the field Mg/Ca-temperature calibration and a typical central Arctic Ocean temperature profile. White circles depict the multicore (MC) and kastenlot (KL) coring sites. All cores were recovered during the SWERUS-C3 expedition, except a single MC obtained during the northern Greenland Petermann-2015 Expedition. Equidistance of the bathymetric contour lines is 50 m. These are drawn until 900 m water depth emphasizing the deepest limit of Atlantic waters. A water column temperature curve from the central Arctic Ocean shows the typical Arctic water masses. Data are from the World Ocean Atlas 2013 database (1955–2012) (Locarnini et al., 2013). They depict vertical temperatures every 1° along the direction of the Lomonosov Ridge with a width of 200 km to provide a view of average temperatures for the Arctic water column. Arctic Ocean bathymetry is after IBCAO data set (Jakobsson et al., 2012) and under ice seabed topography is after BEDMAP from the British Antarctic Survey.

due to seasonally varying influence of Pacific origin waters (Woodgate et al., 2005; Pisareva et al., 2015). This includes both warmer and fresher summer Pacific water inflows, which fuel significantly higher primary productivity compared to the other marginal Arctic shelf seas due to Pacific Ocean sourced nutrients (Astakhov et al., 2015).

2. MATERIAL AND METHODS

2.1. Seafloor sediment and oceanographic sampling

The study is based on 27 sampling stations from the Chukchi Sea Shelf (6), East Siberian Sea Slope (15), Laptev Sea Shelf (1), Lomonosov Ridge (4) and Petermann Fjord (Northern Greenland) (1) (Table 1, Fig. 1). Among these, 23 multicores, 2 kastenlot and 1 piston cores were obtained by icebreaker *Oden* at the edge of the summer sea ice in the eastern Siberian sector of the Arctic Ocean during SWERUS-C3 Expedition Leg 2 (August–September

2014). A multicore from SWERUS-C3 Leg 1 (July–August 2014) was included because it recorded the lowest BWT sampled during the two expedition legs. All the cores and samples are curated at Stockholm University Dept. of Geological Sciences. In the course of this investigation an additional stained *E. clavatum* sample from a multicore taken off northern Greenland from the Petermann Fjord (OD1507-002-MC02, 0–2 cm) became available. This station, sampled during the Petermann Expedition (summer 2015), was helpful in expanding the field temperature range in the *E. clavatum* Mg/Ca-BWT calibration set.

The seafloor sampling stations span water depths of 52–1157 m and temperatures of -1.8 to 0.9 °C, intersecting all three main Arctic Ocean water masses. Oceanographic data (temperature, salinity, total alkalinity, total CO₂ and pH) were sampled during SWERUS-C3 through conductivity, temperature and depth (CTD) casts with attached Niskin bottles that were released to sample bottom water at the coring stations. For the Petermann Fjord site (OD1507-

Table 1

Sample stations used in this study and their field bottom water properties. Site and oceanographic data sources were collected during Expeditions SW = SWERUS-C3 (26 sites) and Petermann-2015 (one site: OD1507-002-MC02). KL = kastenlot, MC = multicore, PC = Piston core. Site locations are: LR, Lomonosov Ridge; HC, Herald Canyon (Chukchi Sea); ESS, Eastern Siberian Sea; LS, Laptev Sea. Carbonate ion data ($\Delta[\text{CO}_3^{2-}]$) was computed using CO2calc Ver. 1.3.0 (Robbins et al., 2010) and utilizing seawater chemistry measurements (see text for details). RB = Rose Bengal (RB) stained samples are considered modern, i.e. alive at time of collection and thus have zero age. CBF = calcareous benthic foraminifera.

Site	Lat (°N)	Lon (°E)	Water depth (m)	Arctic Ocean location	BWT (°C)	Salinity	$\Delta[\text{CO}_3^{2-}]$ ($\mu\text{mol/kg}$)	# RB stained CBF (0–6 cm)
SW L2-1-KL	72.337483	–176.439	73	HC	–1.66	32.89	0.67	–
SW L2-2-KL	72.566766	–175.265	71	HC	–0.72	32.88	–4.27	133
SW L2-2-MC	72.4317	–175.342	56	HC	–0.90	32.61	8.12	115
SW L2-2-PC	72.51658	–175.320	57	HC	–0.90	32.71	8.12	–
SW L2-3-MC	72.3771	–175.786	90	HC	–1.71	32.93	–3.53	50
SW L2-4-MC	72.8609	–175.711	124	HC	–0.26	34.36	–10.35	195
SW L2-8-MC	75.1532	179.873	524	ESS slope	0.28	34.87	45.02	277
SW L2-9-MC	75.0567	–179.820	446	ESS slope	0.45	34.86	47.37	116
SW L2-13-MC	76.186327	–179.278	1118	ESS slope	–0.22	34.89	37.55	78
SW L2-14-MC	76.3529	176.461	733	ESS slope	0.25	34.89	42.50	72
SW L2-15-MC	76.3203	175.881	501	ESS slope	0.52	34.86	46.65	187
SW L2-16-MC	76.512015	176.632	1023	ESS slope	–0.07	34.90	38.06	92
SW L2-18-MC	76.4091	173.879	349	ESS slope	0.74	34.85	46.61	369
SW L2-21-MC	77.579254	163.308	153	ESS slope	–0.10	34.50	25.42	153
SW L2-22-MC	78.223877	164.427	367	ESS slope	0.91	34.87	47.76	104
SW L2-23-MC	78.664367	165.033	522	ESS slope	0.69	34.90	49.99	78
SW L2-24-MC	78.80003	165.382	982	ESS slope	0.02	34.91	39.51	142
SW L2-25-MC	79.226288	152.676	101	ESS slope	–0.87	34.24	28.80	102
SW L2-26-MC	79.742133	154.389	378	ESS slope	0.53	34.86	50.81	189
SW L2-27-MC	79.664634	154.126	276	ESS slope	0.43	34.82	49.99	125
SW L2-28-MC	79.919544	154.354	1145	ESS slope	–0.16	34.91	36.98	112
SW L2-29-MC	81.342771	141.775	910	LR crest	0.02	34.91	42.53	170
SW L2-31-MC	79.920391	143.165	1157	ESS slope-LR	–0.21	34.91	37.70	8
SW L2-32-MC	85.141183	151.590	837	LR crest	–0.01	34.90	43.88	133
SW L2-34-MC	84.27605	148.713	886	LR crest	–0.10	34.90	41.80	321
SW L1-26-MC/I	76.473	132.044	52	LS	–1.82	34.21	29.97	52
OD1507-002-MC02	81.174	–62.062	873	N Greenland	0.30	34.78	–	–

002-MC02), only CTD temperature and salinity data were available (Münchow and Heuzé, 2015). The degree of Δ $[\text{CO}_3^{2-}]$ defined as $[\text{CO}_3^{2-}]_{\text{measured}}$ minus $[\text{CO}_3^{2-}]_{\text{saturation}}$ was calculated using CO2calc Ver. 1.3.0 (Robbins et al., 2010). Program input variables were derived from measurements of total alkalinity, total CO_2 and pH. Additional input parameters were the CO_2 dissociation constants K1 and K2 (Mehrbach et al., 1973) refit by (Dickson and Millero, 1987) (Appendix Table A).

2.2. Benthic foraminifera sampling and faunal analysis

The recovered SWERUS-C3 multicore sediments were immediately frozen after retrieval and sampled in Stockholm post cruise (Table 1). Multicores were sliced into 1-cm thick samples over a depth interval of up to 32 cm (Appendix Table B). The purpose was to observe/include potentially useful infaunal taxa living within seafloor sediments. The extracted sediment samples were immediately wet sieved using deionized water over a 63 μm sieve. The $>63 \mu\text{m}$ size fractions were dosed with Rose Bengal (RB) protein stain and left for a minimum of 14 days according to established methods (Schönfeld et al., 2012). The RB solution was prepared using 2 g of RB dissolved in 1L ethanol (99%). The RB staining colours protoplasm a vivid pink (Fig. 2) (Walton, 1952; Corliss and Emerson, 1990), thus

allowing distinction between foraminiferal specimens that were alive (or recently dead) at the time of sampling, and older ‘fossils’ that are mixed into the surface layer. Once staining was complete, each sample was wet-picked in a Petri dish to better distinguish the pink-stained cytoplasm inside the tests. Representative specimens were imaged using a digital camera mounted to a Leica Microsystems DFC 295 light microscope (Fig. 2). Specimens qualified as ‘stained’ only if all chambers, except the ultimate (youngest), appeared brightly stained. Staining was difficult to assess in thick-shelled porcelaneous taxa (e.g. the miliolid *Q. arctica*), thus it was necessary to break the tests between glass plates to observe stained cytoplasm.

We surveyed the foraminifera taxonomic distributions across the study areas using the RB stained assemblages. All individuals in the 125–500 μm size fraction range were identified to species level and counted (Table 1 and Appendix Table B). Stained individuals were found in the upper 6 cm, thus including both epifaunal (surface living) and infaunal (subsurface living) species. Counts were standardized to a 471 cm^3 volume of sediment (6 cm subsurface sediment depth, 10 cm diameter multicore). The taxonomy, distribution and ecology of Arctic Ocean benthic foraminifera were taken from various sources (Green, 1960; Lagoe, 1977; Scott et al., 1989; Scott and Vilks, 1991; Wollenburg, 1992; Bergsten, 1994; Seidenkrantz, 1995; Wollenburg and

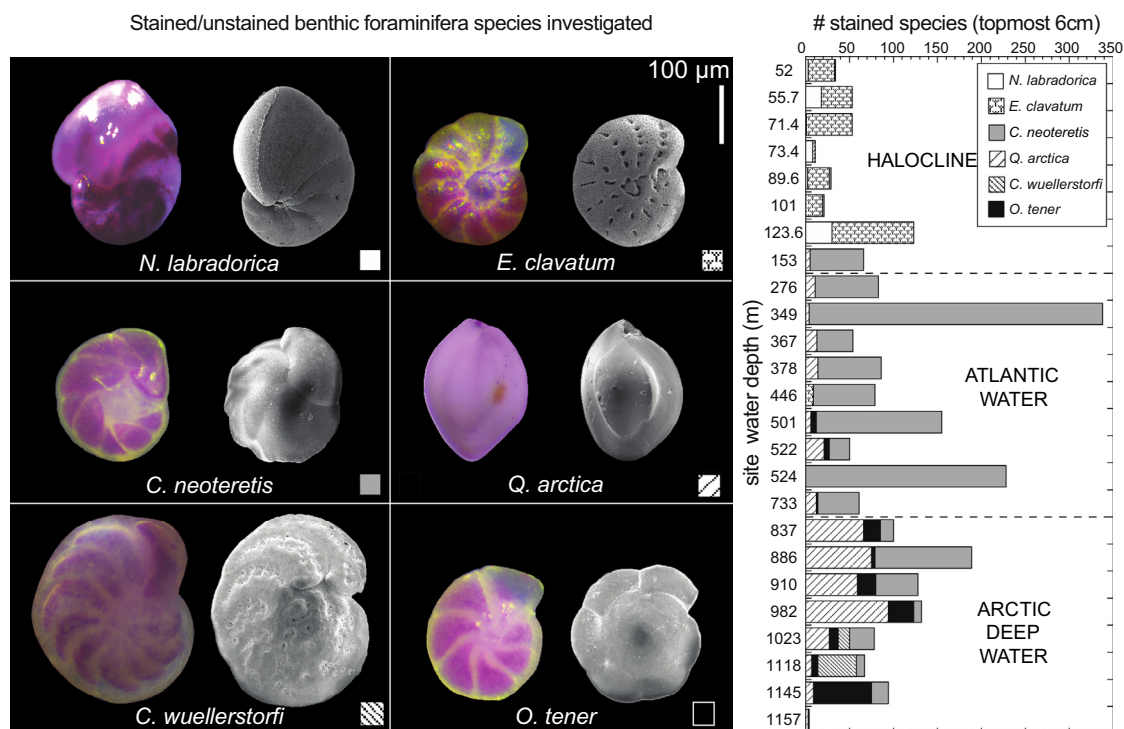


Fig. 2. Representative Rose Bengal stained optical microscope (pink) and scanning electron microscope (grey scale) images of the six foraminiferal species analyzed in this study and their depth and water mass distributions. Scale bar (100 μm) illustrates the average size fraction of the individuals picked for analysis. *N.* = *Nonionella*; *E.* = *Elphidium*; *C.* = *Cassidulina*; *Q.* = *Quinqueloculina*; *C.* = *Cibicides*; *O.* = *Oridorsalis*. Bar plots show the abundance of these species at each site within the uppermost 6 cm of each multicore. Sites are ordered by water depth (depth axis is not to scale). (For interpretation of the references to colour in this figure legend, the reader is referred to the web version of this article.)

Mackensen, 1998a; 1998b; Osterman et al., 1999; Scott et al., 2008).

2.3. Trace metal analysis

Between 3 and 48 monospecific benthic foraminifera were analyzed for trace metals from samples spanning 0–4 cm into the sediment of each multicore. The test size class analyzed varied for each species, reflecting the ‘typical’ per-taxa size range (Table 2). This ‘typical’ size range was defined using the digital measuring tool in the Leica optical-microscope and camera system. Replicate analyses were performed for *N. labradorica* (two sites with two replicates each), *E. clavatum* (four sites with two replicates each) and *C. wuellerstorfi* (one site with two replicates). The tests were crushed between glass plates, inspected under the microscope and impurities remaining in the inner chambers were removed with a wet brush. The test fragments were stored in polypropylene acid-cleaned (10% HCl) Eppendorf safe lock tubes (0.5 ml). The fragments were rigorously cleaned at Cardiff University, applying three clay-removal steps followed by oxidative and reductive steps to remove external metal sources derived from clays, organic matter and metal oxides (Boyle and Keigwin, 1985).

The clean test fragments were dissolved in Optima pure HNO₃ and samples were analyzed against matrix matched standards on a Thermo Element XR high-resolution inductively coupled plasma mass spectrometer (HR ICP-MS) at Cardiff University (Rosenthal et al., 1999; Lear et al., 2002). Long-term analytical precision for Mg/Ca, determined by analysis of consistency standards over the course of a year, is ~1% r.s.d. All data with a Mg signal to noise intensity less than twenty times the blank, and a [Ca] concentration more than 15% different from the standard were rejected. An additional screening step was undertaken to test for contamination by clays and/or metal-oxide coatings (Boyle, 1983; Barker et al., 2003). This was achieved by observing intra-species consistency for some of the other trace metal ratios collected at the same time as Mg/Ca, that are commonly associated with such contamination (Fe/Ca, Al/Ca and Mn/Ca). If the ratios of an individual sample deviate strongly from the typical values, and are significantly higher than previous species-specific indications they would be rejected. The majority of the measured Al/Ca, Fe/Ca and Mn/Ca analysis in hyaline species fell within 300 μmol/mol, 70 μmol/mol and 90 μmol/mol, respectively, with the exception of *N. labradorica* which registered Fe/Ca and Mn/Ca values an order of magnitude higher, in agreement with previous studies (Skirbekk et al., 2016). Likewise, all Al/Ca, Fe/Ca and Mn/Ca were an order of magnitude higher for porcelaneous *Q. arctica*. In cases where Al/Ca, Fe/Ca and Mn/Ca values appeared high, they did not co-vary with Mg/Ca and thus no Mg/Ca data were excluded based on this screening approach. Mg/Ca data taken from previously published studies were adjusted to the full cleaning method by removing 0.1 mmol/mol Mg/Ca (Elderfield et al., 2006; Yu and Elderfield, 2008) (Appendix Table C).

3. RESULTS

3.1. Arctic Ocean seafloor oceanography and water mass properties

Seafloor temperature data obtained from SWERUS-C3 CTD casts (Table 1, Fig. 3), span water depths between 52 and 1157 m and a temperature range of –1.8 to 0.9 °C. Collectively they produce a vertical temperature profile in which the main Arctic water masses can be identified. These include the polar mixed layer (~0 to 50 m), a pronounced halocline (~50 to 200 m), warmer and saltier Atlantic waters (200–900 m) and the more homogeneous Arctic deep waters (900–1200 m) (Fig. 3a).

Temperature, salinity and Δ[CO₃²⁻] co-vary through the depth profile. All show the largest variability in the upper 200 m comprising mixed layer and halocline waters. The measured range of Δ[CO₃²⁻] falls within the range observed previously for the ‘Nordic Sea’ (Elderfield et al., 2006). Similar to BWT, the bottom water Δ[CO₃²⁻] profile is inverted, with lowest values at the surface within halocline depths. Chukchi Sea/Herald Canyon stations (Cores SW-L2-1-KL, -2-MC, -2-KL, -3-MC and -4-MC) show the most depleted Δ[CO₃²⁻], which falls to negative values. The Eastern Siberian slope (SW-L2-21-MC and -25-MC) and Laptev Shelf (SW-L1-26-MC/I) surface values are somewhat higher (25–30 μmol/kg) but are still low compared to the Atlantic layer. Beneath the halocline, temperatures are warmer than the shallowest mixed layer waters by up to 2 °C (from –1.3 to 0.7 °C). Salinity and Δ[CO₃²⁻] are also higher below the halocline (32.6–34.8 psu and –10 to 50 mol/kg respectively), reflecting Atlantic water chemistry and temperature. Arctic deep waters (900–1200 m) are nearly isothermal (less than 1 °C temperature change) and homohaline (34.9 psu). Δ[CO₃²⁻] decreases beneath the Atlantic layer, similar to other ocean basins (Broecker and Peng, 1992), and a previous Arctic study (Jutterström and Anderson, 2005). There is a broad correlation between BWT and Δ[CO₃²⁻] for stations below 200 m (Fig. 4), as would be predicted by typical Δ[CO₃²⁻]/temperature/depth relationships. However, unlike other oceans, our shallowest sites, which largely sit in the uppermost halocline, have low Δ[CO₃²⁻] values, typically <30 μmol/kg, similar to less well ventilated Arctic deep water. When Δ[CO₃²⁻] is above 30 μmol/kg there appears to be less variability (~20 μmol/kg variability), showing a general positive correlation with temperature, while below 30 μmol/kg, where BWT < –0.5 °C, Δ[CO₃²⁻] values are more scattered (~40 μmol/kg variability). In these cases the scatter is likely a consequence of water mass mixing effects, with the extremely low values of SW-L2-4-MC and -1-KL, a consequence of high dissolved CO₂ content in Pacific water and shelf waters (Pisareva et al., 2015; Anderson et al., 2016).

3.2. Spatial and water depth distribution of living benthic foraminifera

‘Live’ RB stained benthic foraminifera were found in all the core-top samples across the sampled depth range with different species showing different depth preferences

Table 2

Arctic benthic foraminifera Mg/Ca results from the topmost 0–3 cm sediments at each site and their respective hydrographic and geochemical characteristics. Calcite saturation state ($\Delta[\text{CO}_3^{2-}]$) was computed using CO2calc Ver. 1.3.0 (Robbins et al., 2010) and utilizing seawater chemistry measurements (see text for details). Note that there are two replicate values for *N. labradorica* in two sites, for *E. clavatum* in four sites and for *C. wuellerstorfi* in one site. RB: Rose Bengal stained.

Benthic foraminifera	Core ID	# RB specimens run (0–4 cm)	Test size (μm)	Water depth (m)	Field BWT ($^{\circ}\text{C}$)	Mg/Ca (mmol/mol)	$\Delta[\text{CO}_3^{2-}]$ ($\mu\text{mol/kg}$)	P (db)	Temp. ($^{\circ}\text{C}$)	Salinity (psu)	TA ($\mu\text{mol/kg}$)	TCO ₂ ($\mu\text{mol/kg}$)	pH	$[\text{CO}_3^{2-}]$ measured ($\mu\text{mol/kgSW}$)	Ω Ca	$[\text{CO}_3^{2-}]$ saturation ($\mu\text{mol/kg}$)
<i>E. clavatum</i>	26-MC/I	20	125–250	52.0	−1.82	0.65	29.97	48	−1.81	34.21	2304.9	2224.4	7.96	71.88	1.72	41.91
<i>E. clavatum</i>	26-MC/I	20	125–250	52.0	−1.82	0.52	29.97	48	−1.81	34.21	2304.9	2224.4	7.96	71.88	1.72	41.91
<i>E. clavatum</i>	2-KL1	13	125–250	71.4	−0.72	0.79	−4.27	70	−1.55	32.7	2251.4	2254.4	7.68	37.56	0.9	41.83
<i>E. clavatum</i>	2-KL1	36	125–250	71.4	−0.72	0.59	−4.27	70	−1.55	32.7	2251.4	2254.4	7.68	37.56	0.9	41.83
<i>E. clavatum</i>	2-PC1	35	125–250	57.0	−0.90	0.75	8.12	50	−0.89	32.6	2246.2	2214	7.8	49.77	1.2	41.65
<i>E. clavatum</i>	2-MC1-4	19	125–250	55.7	−0.90	0.68	8.12	50	−0.89	32.6	2246.2	2214	7.8	49.77	1.2	41.65
<i>E. clavatum</i>	3-MC1-4	15	125–250	89.6	−1.71	0.55	−3.53	89.1	−1.71	32.93	2260	2260.3	7.68	38.51	0.92	42.04
<i>E. clavatum</i>	3-MC1-5	13	125–250	89.6	−1.71	0.75	−3.53	89.1	−1.71	32.93	2260	2260.3	7.68	38.51	0.92	42.04
<i>E. clavatum</i>	4-MC1-4	25	125–250	123.6	−0.26	0.64	−10.35	114.7	−0.26	34.37	2292	2320	7.56	32.26	0.76	42.61
<i>E. clavatum</i>	4-MC1-5	16	125–250	123.6	−0.26	0.67	−10.35	114.7	−0.26	34.37	2292	2320	7.56	32.26	0.76	42.61
<i>E. clavatum</i>	OD1507-002-MC02	48	125–250	873.0	0.30	1.06	–	–	0.30	34.78	–	–	–	–	–	–
<i>N. labradorica</i>	26-MC/I	3	350–425	52.0	−1.82	1.12	29.97	48	−1.81	34.21	2304.9	2224.4	7.96	71.88	1.72	41.91
<i>N. labradorica</i>	1-KL1	3	350–425	73.4	−1.66	1.30	0.67	70.3	−1.66	32.8	2257.4	2245.1	7.73	42.53	1.02	41.86
<i>N. labradorica</i>	2-MC1-4	10	250–350	55.7	−0.90	1.25	8.12	50	−0.89	32.6	2246.2	2214	7.8	49.77	1.2	41.65
<i>N. labradorica</i>	2-MC1-5	3	350–425	55.7	−0.90	1.11	8.12	50	−0.89	32.6	2246.2	2214	7.8	49.77	1.2	41.65
<i>N. labradorica</i>	3-MC1-5	4	350–425	89.6	−1.71	1.30	−3.53	89.1	−1.71	32.93	2260	2260.3	7.68	38.51	0.92	42.04
<i>N. labradorica</i>	4-MC1-4	10	250–350	123.6	−0.26	1.24	−10.35	114.7	−0.26	34.37	2292	2320	7.56	32.26	0.76	42.61
<i>N. labradorica</i>	4-MC1-5	7	250–350	123.6	−0.26	1.31	−10.35	114.7	−0.26	34.37	2292	2320	7.56	32.26	0.76	42.61
<i>C. neoteretis</i>	8-MC1-4	21	125–250	524	0.28	1.078	45.02	522.8	0.34	34.87	2303.05	2183.1	8.05	91.63	1.97	46.61
<i>C. neoteretis</i>	9-MC1-4	20	125–250	446	0.45	1.090	47.37	437.75	0.56	34.86	2299.65	2174.4	8.03	91.73	2.07	44.36
<i>C. neoteretis</i>	13-MC1-4	18	125–250	1118	−0.22	1.100	37.55	1112.3	−0.27	34.89	2300.7	2180.3	8	90.35	1.71	52.81
<i>C. neoteretis</i>	14-MC1-4	20	125–250	733	0.25	0.971	42.50	734.5	0.21	34.89	2304.1	2184	8.01	91.25	1.87	48.74
<i>C. neoteretis</i>	15-MC1-4	20	125–250	501	0.52	0.987	46.65	504.6	0.5	34.86	2304.2	2181.8	8.02	93.07	2.01	46.42
<i>C. neoteretis</i>	16-MC1-4	20	125–250	1023	−0.07	1.160	38.06	1001.2	−0.12	34.9	2304.7	2186.4	8	89.63	1.74	51.57
<i>C. neoteretis</i>	18-MC1-4	28	125–250	349	0.74	0.998	46.61	342.42	0.73	34.85	2299.3	2180.5	8.01	91.46	2.04	44.86
<i>C. neoteretis</i>	21-MC2-4	27	125–250	159	−0.10	1.040	25.42	154.9	−0.11	34.5	2293	2220	7.9	68.43	1.59	43.01
<i>C. neoteretis</i>	22-MC1-4	28	125–250	367	0.91	1.068	47.76	363.4	0.89	34.87	2304.2	2183.1	8.01	92.82	2.06	45.06

Benthic foraminifera	Core ID	# RB specimens run (0–4 cm)	Test size fraction (µm)	Water depth (m)	Field BWT (°C)	Mg/Ca (mmol/mol)	$\Delta[\text{CO}_3^{2-}]$ (µmol/kg)	P (db)	Temp. (°C)	Salinity (psu)	TA (µmol/kg)	TCO ₂ (µmol/kg)	pH	CO ₃ ²⁻ measured (µmol/kgSW)	Ω Ca	CO ₃ ²⁻ saturation (µmol/kg)
<i>C. neoteretis</i>	23-MC1-4	20	125–250	522	0.69	1.193	49.99	495.7	0.67	34.9	2302.6	2174.2	8.03	96.33	2.08	46.33
<i>C. neoteretis</i>	24-MC1-4	18	125–250	982	0.02	1.070	39.51	971.8	−0.03	34.91	2303.9	2183.6	8	90.76	1.77	51.25
<i>C. neoteretis</i>	26-MC1-4	23	125–250	378	0.53	1.196	50.81	377.6	0.53	34.86	2297.95	2170.3	8.04	96.01	2.12	45.2
<i>C. neoteretis</i>	27-MC1-4	22	125–250	276	0.43	1.033	49.99	270.4	0.39	34.81	2301.1	2177.4	8.03	94.14	2.13	44.16
<i>C. neoteretis</i>	29-MC1-4	21	125–250	910	0.02	0.910	42.53	851.6	−0.01	34.91	2302.5	2179.3	8.01	92.51	1.85	49.98
<i>C. neoteretis</i>	34-MC1-4	30	125–250	886	−0.10	0.842	41.80	888.2	−0.13	34.9	2306.4	2183.8	8.01	92.17	1.83	50.36
<i>Q. arctica</i>	13-MC1-4	4	250–425	1118	−0.22	20.264	37.55	1112.3	−0.27	34.89	2300.7	2180.3	8	90.35	1.71	52.81
<i>Q. arctica</i>	15-MC1-4	3	250–425	501	0.52	41.851	46.65	504.6	0.5	34.86	2304.2	2181.8	8.02	93.07	2.01	46.42
<i>Q. arctica</i>	16-MC1-4	3	250–425	1023	−0.07	22.553	38.06	1001.2	−0.12	34.9	2304.7	2186.4	8	89.63	1.74	51.57
<i>Q. arctica</i>	18-MC1-4	3	250–425	349	0.74	75.085	46.61	342.42	0.73	34.85	2299.3	2180.5	8.01	91.46	2.04	44.86
<i>Q. arctica</i>	21-MC2-4	3	250–425	153	−0.10	74.220	25.42	154.9	−0.11	34.5	2293	2220	7.9	68.43	1.59	43.01
<i>Q. arctica</i>	22-MC1-4	4	250–425	367	0.91	53.742	47.76	363.4	0.89	34.87	2304.2	2183.1	8.01	92.82	2.06	45.06
<i>Q. arctica</i>	23-MC1-4	5	250–425	522	0.69	71.181	49.99	495.7	0.67	34.9	2302.6	2174.2	8.03	96.33	2.08	46.33
<i>Q. arctica</i>	24-MC1-4	5	250–425	982	0.02	22.708	39.51	971.8	−0.03	34.91	2303.9	2183.6	8	90.76	1.77	51.25
<i>Q. arctica</i>	26-MC1-4	3	250–425	378	0.53	69.776	50.81	377.6	0.53	34.86	2297.95	2170.3	8.04	96.01	2.12	45.2
<i>Q. arctica</i>	27-MC1-4	3	250–425	276	0.43	74.948	49.99	270.4	0.39	34.81	2301.1	2177.4	8.03	94.14	2.13	44.16
<i>Q. arctica</i>	28-MC1-4	3	250–425	1145	−0.16	18.889	36.98	1147.5	−0.24	34.91	2307.7	2187.8	8	90.2	1.7	53.21
<i>Q. arctica</i>	29-MC1-4	4	250–425	910	0.02	59.880	42.53	851.6	−0.01	34.91	2302.5	2179.3	8.01	92.51	1.85	49.98
<i>Q. arctica</i>	34-MC1-4	3	250–425	886	−0.10	39.397	41.80	888.2	−0.13	34.9	2306.4	2183.8	8.01	92.17	1.83	50.36
<i>O. tener</i>	23-MC1-4	16	125–250	522	0.69	1.67	49.99	495.7	0.67	34.9	2302.6	2174.2	8.03	96.33	2.08	46.33
<i>O. tener</i>	24-MC1-4	16	125–250	982	0.02	1.50	39.51	971.8	−0.03	34.91	2303.9	2183.6	8	90.76	1.77	51.25
<i>O. tener</i>	28-MC1-4	24	125–250	1145	−0.16	1.43	36.98	1147.5	−0.24	34.91	2307.7	2187.8	8	90.2	1.7	53.21
<i>O. tener</i>	29-MC1-4	16	125–250	910	0.02	1.74	42.53	851.6	−0.01	34.91	2302.5	2179.3	8.01	92.51	1.85	49.98
<i>O. tener</i>	32-MC1-4	15	125–250	837	−0.01	1.78	43.88	888.2	−0.13	34.9	2306.4	2183.8	8.01	92.17	1.83	50.36
<i>C. wuellerstorfi</i>	13-MC1-4	7	350–425	1118	−0.22	1.32	37.55	1112.3	−0.27	34.89	2300.7	2180.3	8	90.35	1.71	52.81
<i>C. wuellerstorfi</i>	13-MC1-4	6	350–425	1118	−0.22	1.15	37.55	1112.3	−0.27	34.89	2300.7	2180.3	8	90.35	1.71	52.81
<i>C. wuellerstorfi</i>	16-MC1-4	9	350–425	1023	−0.07	1.48	38.06	1001.2	−0.12	34.9	2304.7	2186.4	8	89.63	1.74	51.57

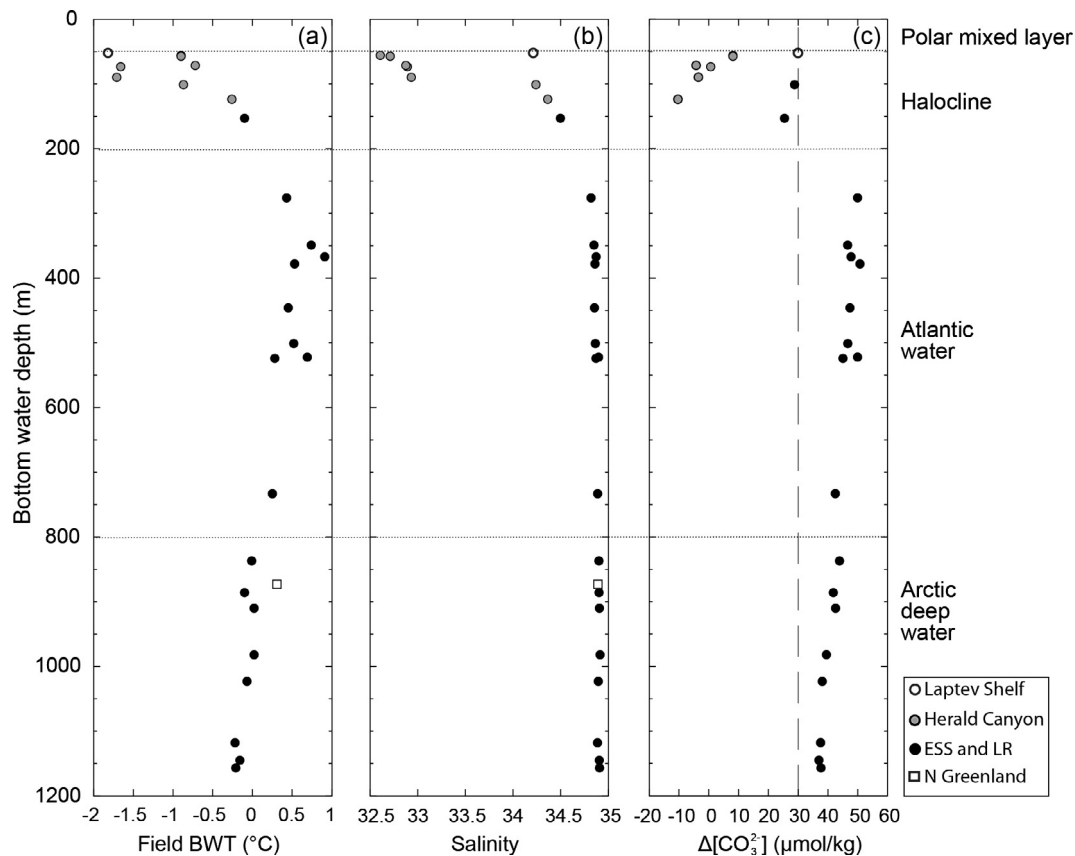


Fig. 3. Bottom water oceanographic data across the 27 sites investigated in this study. (a) Bottom water temperature (BWT), (b) salinity, (c) calculated seawater $\Delta[\text{CO}_3^{2-}]$. See Table 1 for data source. The sites collectively span the three main water masses found in the Arctic Ocean, the approximate depth boundaries of which are depicted by horizontal lines. The vertical dashed line in (c) at $30 \mu\text{mol/kg}$ identifies the threshold where $\Delta[\text{CO}_3^{2-}]$ loses the trend with temperature (Fig. 4) and could influence measured Mg/Ca more strongly. No $\Delta[\text{CO}_3^{2-}]$ data was available for the Northern Greenland site (open square). Grey circles represent Chukchi Shelf sites (Herald Canyon). This region, which is bathed by 'old', nutrient-rich Pacific waters entering the Arctic across the Bering Strait, has the greatest $\Delta[\text{CO}_3^{2-}]$ and salinity variability with small depth differences. Black-filled circles show bottom water samples from ESS = Eastern Siberian Shelf/slope and LR = Lomonosov Ridge.

(Table 1, Figs. 2 and 5). All studied species build low Mg tests except *Q. arctica*, which has a high Mg-calcite test. Of the six species, three are epifaunal (*Q. arctica*, *C. wuellerstorfi* and *O. tener*) while the others (*C. neoteretis*, *N. labradorica*, *E. clavatum*) are deep infaunal (Wollenburg and Mackensen, 1998b; Murray, 2006). In this sample set, size fractions are 125–250 μm for *E. clavatum*, *C. neoteretis* and *O. tener*; and 250–425 μm for *N. labradorica*, *Q. arctica* and *C. wuellerstorfi* (Fig. 2). Five of these six taxa (or a closely related species belonging to the same genus) have been the subject of previous Mg/Ca-BWT investigations outside of the Arctic Ocean, thus allowing new calibrations across a wider temperature range (–1.8 to 25.7 °C).

The Arctic benthic foraminifera distribution patterns are thought to be primarily controlled by food availability (Wollenburg, 1995). Assemblages from the shallowest sites (halocline waters), on the Chukchi, East Siberian and Laptev shelves have the highest abundances of the hyaline infaunal species *E. clavatum* followed by *N. labradorica*. Both species have a wide global distribution and are considered to prefer shelf seas with high primary production and

dominate in deep water areas of European fjords (Murray, 2006). They are deposit feeders protected from strong bottom currents by their infaunal habitat (Wollenburg, 1992; Murray, 2006). *Elphidium clavatum* is known to tolerate environmental stress (Schafer et al., 1975; Dabbous and Scott, 2012) that in the Herald Canyon will be related to strong salinity shifts brought by its location at the seasonal sea ice margin, and to dysoxic low $\Delta[\text{CO}_3^{2-}]$ bottom waters of Pacific origin.

Sites located on the East Siberian slope and at shallow depths on the Lomonosov Ridge (~600 to 800 m), are bathed by warmer and saltier Atlantic waters and contain higher proportions of *C. neoteretis* (also known as *Islandiella teretis*). This infaunal species is typical of Arctic inner shelf to bathyal environments where Atlantic water flows (Seidenkrantz, 1995; Scott et al., 2008; Lazar et al., 2016). *Cassidulina neoteretis* is the most abundant of all studied species and habits the widest depth ranges. It shows a pronounced peak in abundance at 280–350 m water depth coincident with the upper Atlantic water. It is dominant (>50%) at stations 8-MC, 9-MC, 14-MC, 15-MC, 18-MC,

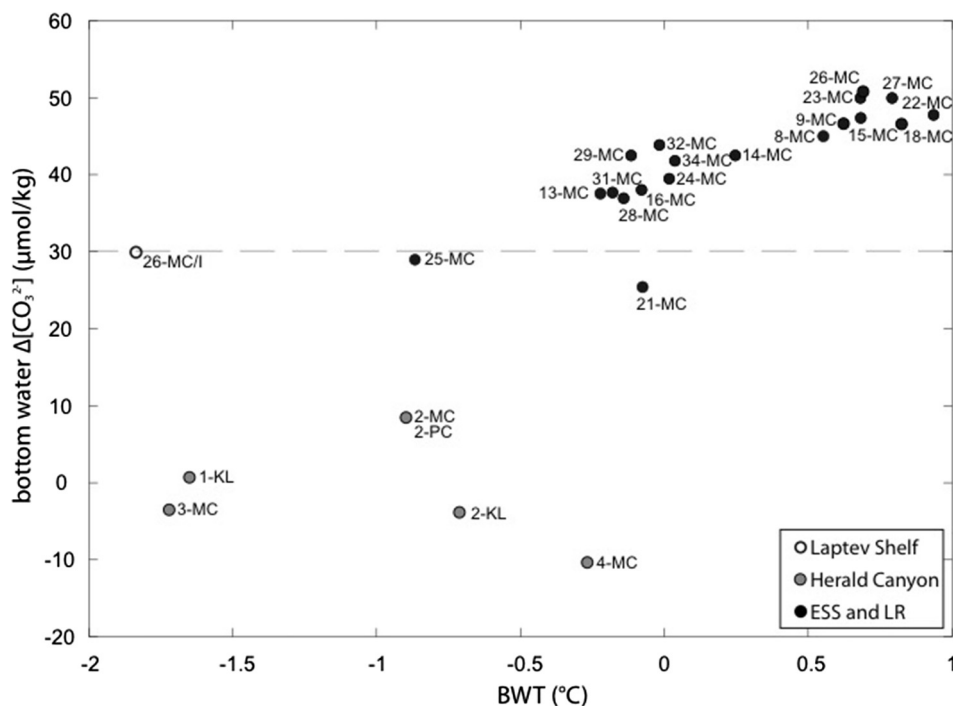


Fig. 4. Bottom water $\Delta[\text{CO}_3^{2-}]$ and temperature relationship at the SWERUS-C3 Arctic Ocean study sites spanning BWT below 1 °C. See Table 1 for site information. An almost linear $\Delta[\text{CO}_3^{2-}]$ -BWT trend is observed and is disrupted at 30 $\mu\text{mol/kg}$, depicted as a dashed line. This limit characterizes the hypothesized 30 $\mu\text{mol/kg}$ threshold, below which $\Delta[\text{CO}_3^{2-}]$ could influence test Mg/Ca. Our halocline sites fall into this category. Note that no $\Delta[\text{CO}_3^{2-}]$ data was available for the Northern Greenland site.

21-MC, 22-MC, 26-MC, 27-MC and 34-MC (Fig. 5). Below the Atlantic layer in Arctic deep waters (>800 m), *Q. arctica*, *O. tener* and *C. wuellerstorfi* are the most abundant species, consistent with previous observations (Scott and Vilks, 1991; Bergsten, 1994; Scott et al., 2008). *Quinqueloculina arctica*, common in Arctic and cold North Atlantic subsurface waters, is the most common species at sites 24-MC, 29-MC, 31-MC and 32-MC, where water depths range between 837 and 1157 m. The presence of epifaunal *C. wuellerstorfi* at depths of ~1000 m (13-MC and 16-MC) might reflect more oligotrophic conditions in this region (Altenbach and Sarnthein, 1989). *Oridorsalis tener* appears in small numbers at water depths around 500 m (15-MC and 23-MC) and becomes dominant at 1145 m (25-MC). This is consistent with previous studies illustrating that this species has a preference for Atlantic waters sitting at bathyal to abyssal depths. Outside the Arctic Ocean many authors do not recognize or differentiate *O. tener* from the better known close relative *O. umbonatus* (Osterman et al., 1999). According to some, *O. tener* is considered epifaunal while *O. umbonatus* is thought to be shallow infaunal (Murray, 2006).

3.3. Benthic foraminifera Mg/Ca and bottom water temperature

None of the six species occupy the full bathymetric or temperature range. Thus, while the maximum vertical Arctic Ocean temperature range is ~3 °C (Fig. 3), the narrow preferred depth of the individual species means our

monospecific Mg/Ca-BWT data span even narrower temperature ranges. The ranges captured are 2.12 °C in *E. clavatum*, 1.56 °C in *N. labradorica*, 1.45 °C in *Q. arctica*, 1.38 °C in *C. neoteretis*, 1.28 °C in *O. tener* and 0.15 °C in *C. wuellerstorfi*. Measured Mg/Ca in hyaline *E. clavatum*, *N. labradorica*, *C. neoteretis*, *O. tener* and *C. wuellerstorfi* range between 0.5 and 1.8 mmol/mol.

Mg/Ca in *E. clavatum* (7 stations, n = 11) varies between 0.52 and 1.06 mmol/mol and spans a BWT range of -1.82 to 0.3 °C (Fig. 6a). The warmest data point, which comes from the Petermann Fjord (northern Greenland), fits with the overall trend. For *N. labradorica* (5 stations, n = 7), also common in the halocline, Mg/Ca of 1.11–1.31 mmol/mol resulted over a temperature gradient of -1.82 to -0.26 °C (Fig. 6b). Mg/Ca of *N. labradorica* is ~0.6 mmol/mol higher than *E. clavatum* Mg/Ca from the same locality, consequence of the “vital effect”. *Cassidulina neoteretis*, which is most common in the warmer waters of the Atlantic layer (15 stations, n = 15), has Mg/Ca values that vary between 0.84 and 1.20 mmol/mol for a BWT range of -0.47 to 0.91 °C (Fig. 6c). Like other species producing high-Mg ‘porcelaneous tests’ (Toyofuku et al., 2000), the measurements on stained *Q. arctica* (13 stations, n = 13) show Mg/Ca up to 40 times higher than hyaline taxa, with values of 18.89–75.08 mmol/mol over a -0.54 to 0.91 °C BWT range (Fig. 6d). There are a small number of deep-water stations where *O. tener* and *C. wuellerstorfi* were present. In *O. tener* (5 stations, n = 5), Mg/Ca is 1.43–1.78 mmol/mol over a BWT range of -0.59 to 0.69 °C (Fig. 6e). The three *C. wuellerstorfi* data points (2 stations, n = 3)

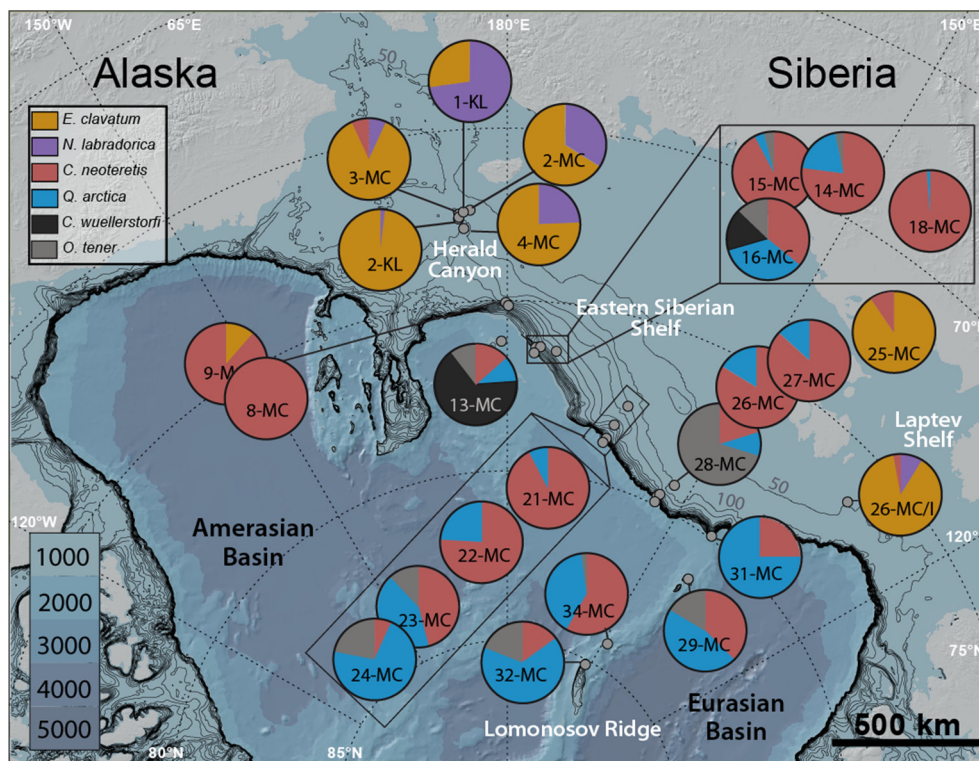


Fig. 5. Spatial distribution and proportions of the six species used in this study as observed in ‘live’ benthic foraminiferal assemblages (Rose Bengal stained) from the SWERUS-C3 25 multicore (MC) and kastenlot (KL) core top sites (grey circles). Counts were made on the >125 μm stained species found in the topmost 6 cm of each multicore. The Northern Greenland site is not depicted because species counts were not available. At these sites, assemblage composition is controlled by water depth, different species or combinations of species preferring the different Arctic Ocean layers: *N. labradorica* and *E. clavatum* are restricted to the shelves; *C. neoteretis* and *Q. arctica* prefer continental slope and top ridge settings; *O. tener* and *C. wuellerstorfi* are most common in deeper sites. Geographic regions where the multicores were retrieved Herald Canyon, Eastern Siberian Shelf and slope, Laptev Shelf and Lomonosov Ridge. Equidistance of the contour lines is 50 m. These are present down to 900 m of water depth representing the lower limit of Atlantic water flowing into the Arctic basin.

show Mg/Ca of 1.15–1.48 mmol/mol and a BWT of -0.22 to -0.07 °C (Fig. 6f). Linear regressions are tentatively shown in Fig. 6 and Table 3 for discussion purposes. They are not intended for use as palaeotemperature calibrations, except for the Arctic *E. clavatum* dataset which, having the widest range of field BWT, produces a reasonable correlation with Mg/Ca.

3.4. Mg/Ca and bottom water carbonate ion concentration ($\Delta[\text{CO}_3^{2-}]$)

Similar to Arctic Ocean temperature structure, the $\Delta[\text{CO}_3^{2-}]$ pattern is atypical compared to other oceans, with surface waters having the lowest $\Delta[\text{CO}_3^{2-}]$ (Fig. 3c). Thus, most of the sites sitting in halocline waters from the Herald Canyon have <0 $\mu\text{mol/kg}$ in bottom water $\Delta[\text{CO}_3^{2-}]$ as a consequence of Pacific origin bottom waters bathing the sites that differ from the dominant Arctic water masses by having lower salinity, $\Delta[\text{CO}_3^{2-}]$, lower oxygen concentration and higher nutrients (Walsh et al., 1989; Chierici and Fransson, 2009). In contrast, most of the Arctic Ocean sites on the eastern shelves, slopes and ridges have oversaturated waters with respect to calcite, as observed in other studies (Jutterström and Anderson, 2005). Mg/Ca data from

monospecific hyaline species show no correlation with bottom water $\Delta[\text{CO}_3^{2-}]$ (Fig. 7a, b, c, e and f), whereas Mg/Ca *Q. arctica* shows a clear positive Mg/Ca- $\Delta[\text{CO}_3^{2-}]$ correlation ($r^2 = 0.77$, $n = 13$; regression not shown) over much of the data range, excluding station 21-MC, which shows Pacific water $\Delta[\text{CO}_3^{2-}]$ values of 26 $\mu\text{mol/kg}$ (Fig. 7d).

4. DISCUSSION

The goal of this study was to explore the application of benthic foraminifera Mg/Ca palaeothermometry in the Arctic Ocean and to expand the scarce Mg/Ca data found in benthic foraminifera living at the cold end of the temperature scale. The results represent the most extensive set of physical and chemical field constraints coupled with benthic foraminifera Mg/Ca available to date in the Arctic Ocean, and, hence, provide a unique opportunity for comparison with existing global Mg/Ca-BWT datasets and calibrations.

4.1. Arctic benthic foraminifera Mg/Ca: challenges at the cold end

Previous studies on the thermodynamic controls on Mg incorporation into benthic foraminiferal calcite suggest the

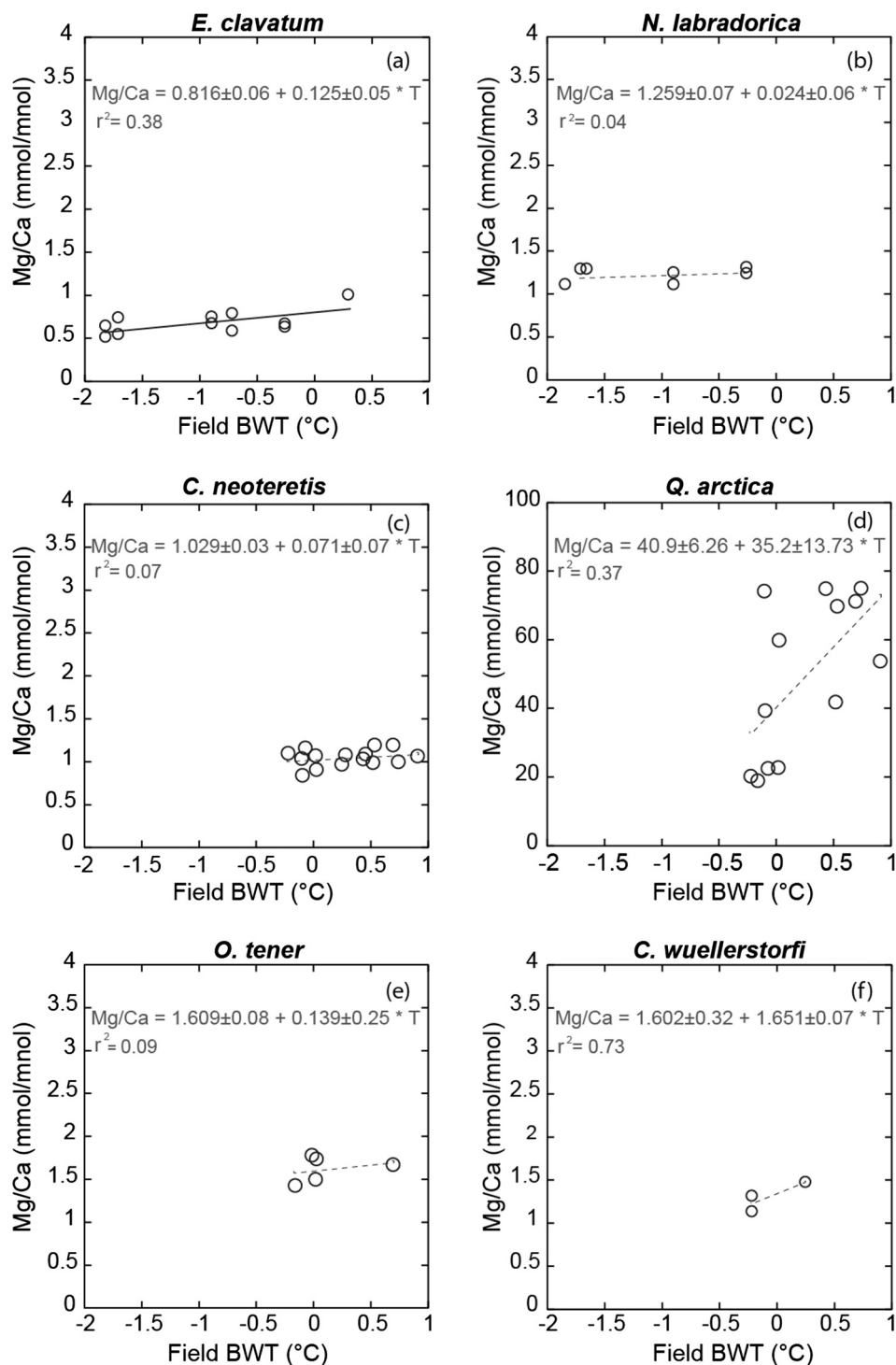


Fig. 6. Benthic foraminifera Mg/Ca data for the six species investigated in this study plotted against field bottom water temperature (BWT). Mg/Ca values of *Q. arctica* (d) are an order of magnitude higher than all other species due to the characteristic high-Mg calcite tests. Dashed linear fits and the associated equations are included to facilitate discussion but are not intended for use as paleotemperature calibrations, the exception being *E. clavatum* having the widest BWT ranges of all the species. Analytical error for Mg/Ca (0.1 mmol/mol) is equivalent to the height of the symbols.

relationship to be either linear (e.g. Toyofuku et al., 2000; Marchitto et al., 2007) or exponential (e.g. Rosenthal et al., 1997; Lear et al., 2002), the latter implying reduced

Mg sensitivity at low temperatures. The conditions that characterize the Arctic Ocean include the coldest end of the global ocean temperature spectrum (down to -2 °C),

Table 3

Comparison of the new and existing Mg/Ca-BWT regression fits for the 6 taxa investigated in this study. The compiled datasets are constructed based on compiled data from sites with no $\Delta[\text{CO}_2^-]$ effect (as described in each study). For published data based on samples that did not receive the full foraminiferal cleaning procedure Mg/Ca values were adjusted by subtracting 0.1 mmol/mol. In bold are the equations favored in this study and illustrated in Fig. 8. Data sources for all the compiled data, showing sample locations and Mg/Ca corrections are presented in Appendix, Table C.

Benthic foraminifera	Reference	n	A	B	R ²	Mg/Ca range (mmol/mol)	BWT (°C)
<i>Linear fit, Mg/Ca = (A * BWT) + B</i>							
<i>E. clavatum</i>	This study (Fig. 8a)	11	0.125	0.816	0.38	0.52–1.06	–1.82 to 0.3
<i>N. labradorica</i>	This study	7	0.024	1.259	0.04	1.11–1.31	–1.82 to –0.26
<i>N. labradorica</i>	Skirbekk et al. (2016) (autumn)	12	0.088	1.345	0.44	1.36–1.69	0.78–3.9
<i>N. labradorica</i>	Compilation	19	0.090	1.344	0.87	1.11–1.69	–1.71 to 3.9
<i>C. neoteretis</i>	This study	15	0.071	1.023	0.07	0.84–1.20	–0.47 to 0.91
<i>C. neoteretis</i>	Kristjánsdóttir et al. (2007)	10	0.093	0.840	0.90	0.93–1.38	0.22–6.25
<i>C. neoteretis</i>	Compilation	25	0.049	1.011	0.62	0.84–1.38	0.96–5.47
<i>Q. arctica</i>	This study	13	35.198	40.882	0.37	18.89–75.08	–0.54 to 0.91
<i>Q. yabei</i>	Toyofuku et al. (2000)	11	1.730	77.640	0.83	95.20–126.10	11.70–25.70
<i>O. tener</i>	This study	5	0.139	1.609	0.09	1.43–1.78	–0.59 to 0.69
<i>O. umbonatus</i>	Healey et al. (2008)	24	0.449	0.773	0.67	1.25–2.60	0.85–3.8
<i>O. umbonatus</i>	Lear et al. (2010)	21	0.12	1.200	0.9	1.11–1.88	–0.6 to 3.7
<i>O. tenerlumbonatus</i>	Compilation	83	0.195	1.309	0.64	1.01–3.96	–0.6 to 10.4
<i>C. wuellerstorfi</i>	This study	3	1.651	1.602	0.73	1.32–1.48	–0.22 to –0.07
<i>C. wuellerstorfi</i>	Healey et al. (2008)	33	0.295	0.670	0.90	0.79–2.05	0.95–3.8
<i>C. lobatulus</i>	Quillmann et al. (2012)	38	0.116	1.20	0.9	1.03–2.41	–0.33 to 9.50
<i>Exponential fit, Mg/Ca = B * e^(A * BWT)</i>							
<i>E. clavatum</i>	This study	11	0.164	0.799	0.40	0.52–1.06	–1.82 to 0.3
<i>N. labradorica</i>	Compilation (Fig. 8b)	19	0.062	1.334	0.88	1.11–3.42	–1.71 to 3.9
<i>C. neoteretis</i>	Kristjánsdóttir et al. (2007)	10	0.082	0.864	0.90	0.93–1.38	0.22–6.25
<i>C. neoteretis</i>	Compilation (Fig. 8c)	25	0.042	1.009	0.62	0.84–1.38	–0.47 to 5.47
<i>O. umbonatus</i>	Lear et al. (2002)	16	0.114	1.008	0.40	1.09–3.43	0.8–9.9
<i>O. umbonatus</i>	Rathmann et al. (2004)	6	0.09	1.528	–	1.91–3.96	2.9–10.4
<i>O. umbonatus</i>	Healey et al. (2008)	24	0.252	0.988	0.67	1.25–2.60	0.85–3.8
<i>O. umbonatus</i>	Tisserand et al. (2013)	12	0.110	1.360	0.53	2.26–3.1	4.17–6.06
<i>O. tenerlumbonatus</i>	Compilation (Fig. 8e)	83	0.102	1.317	0.65	1.01–3.96	–0.6 to 10.4
<i>C. wuellerstorfi</i>	Martin et al. (2002)	27	0.309	0.448	0.81	0.68–1.46	1.8–3
<i>C. wuellerstorfi</i>	Healey et al. (2008)	33	0.230	0.781	0.91	0.79–2.05	0.95–3.8
<i>C. wuellerstorfi</i>	Raitzsch et al. (2008)	44	0.145	0.830	0.89	0.84–2.02	0.39–3.88
<i>C. wuellerstorfi</i>	Tisserand et al. (2013)	34	0.19	0.820	0.73	1.8–3.91	4.17–6.06
<i>C. wuellerstorfi</i>	Compilation (Fig. 8f)	200	0.118	1.043	0.43	0.92–3.81	–1.15 to 6.06
<i>C. lobatulus</i>	Quillmann et al. (2012)	38	0.069	1.240	0.89	1.03–2.41	–0.33 to 9.50
<i>C. wuellerstorfi</i> / <i>lobatulus</i>	Compilation (Fig. 8f)	238	0.092	1.130	0.45	0.92–3.81	–1.15 to 9.50

the narrowest vertical temperature range (3 °C) and the flattest part of the exponential Mg/Ca-BWT sensitivity curve. Hence, the slopes of the regression lines for the Arctic datasets are low (i.e. large temperature range for little change in Mg/Ca). With the exception of *E. clavatum*, these should therefore not be used for palaeothermometry on their own.

There are a variety of potential reasons why pure Arctic-only calibrations are challenging. First, there is the question of whether our measured field BWT are representative of the conditions under which the analyzed foraminifera calcified. In other words, how much seasonal variability is there in BWT and when does calcification occur? We have largely used the CTD temperature data collected at the time of coring, i.e. in late summer August–September 2014. We consider these temperatures and season an appropriate match for *N. labradorica* and *E. clavatum*, which previous studies on fjordal environments from Svalbard and the Swedish west coast have shown grow rapidly at the end of the summer when shelf bottom waters are at their warmest

(Gustafsson and Nordberg, 1999; Gustafsson and Nordberg, 2001; Skirbekk et al., 2016). Seasonal variations in BWT at the depths of the study sites are on the order of ~1 °C, and thus within the Mg/Ca-BWT error, even at the shallowest studied depths of the Laptev and Chukchi Sea sites (Rudels, 2009; Dmitrenko et al., 2009; Luchin and Panteleev, 2014). Thus, we conclude that seasonal BWT changes could account for ‘noise’ on the order of fractions of a degree in our shallower sites (<200 m water depth) but would be insignificant in deeper sites.

Benthic foraminifera life span and peak growth/calcification season in the studied Arctic setting is also uncertain. Predictions range from months to several years and this is likely species and environment dependent (Myers, 1938; Boltovskoy and Wright, 1976; Corliss and Silva, 1993; Debenay et al., 1996; Gustafsson and Nordberg, 1999; 2001; Skirbekk et al., 2016). Moreover, the precise timing of mineralization is uncertain. Indications are that calcification is seasonal in the Arctic. Some studies link the main

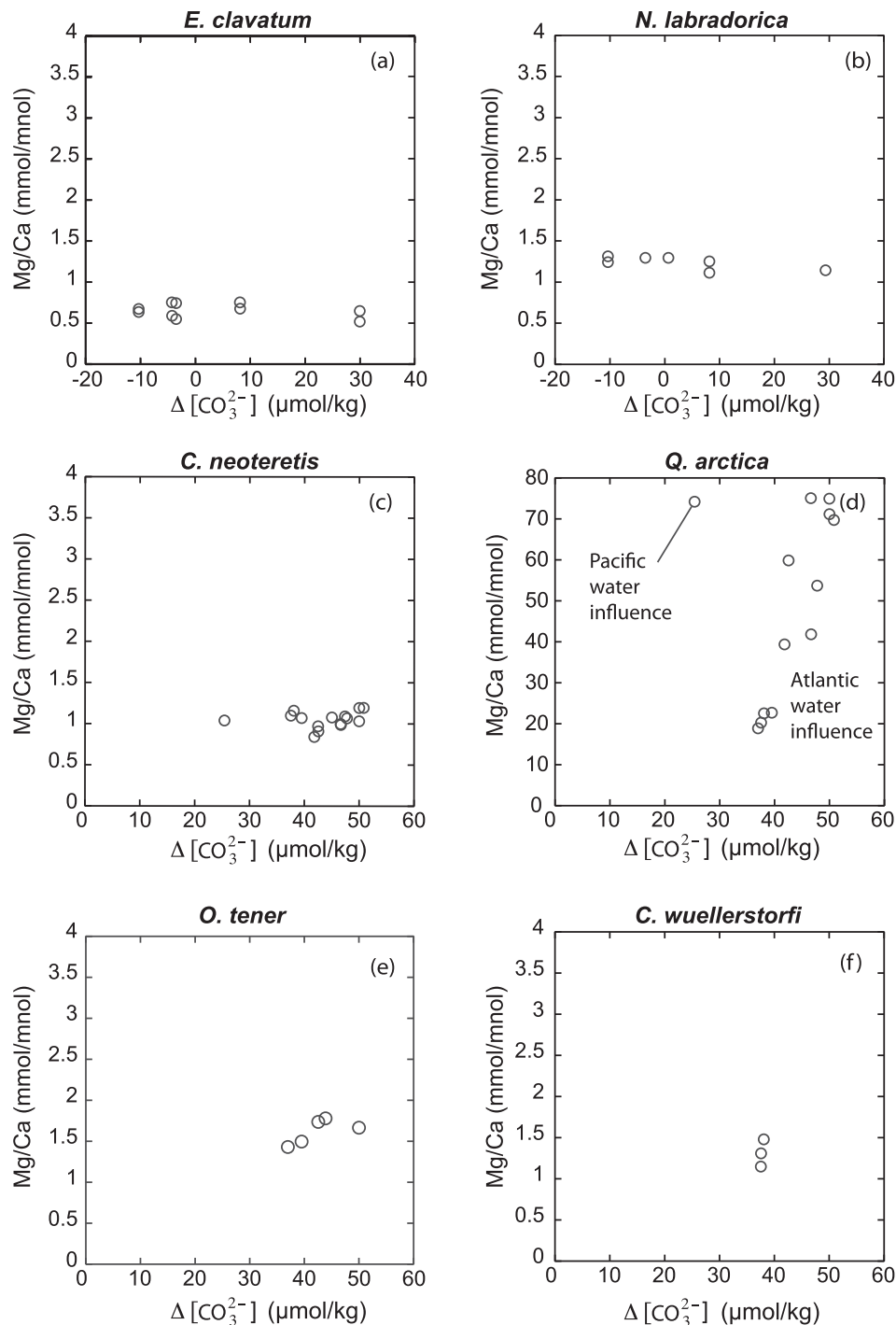


Fig. 7. Benthic foraminifera Mg/Ca data compared to field bottom water $\Delta[\text{CO}_3^{2-}]$. *Quinqueloculina arctica* (d) is the only species showing a positive Mg/Ca relationship to $\Delta[\text{CO}_3^{2-}]$. Shelf sites at water depths <200 m experience wide variability in $\Delta[\text{CO}_3^{2-}]$. The resident shelf species (a) and (b) Mg/Ca results do not show significant relationships with $\Delta[\text{CO}_3^{2-}]$. In (a), the Northern Greenland site data point is not available. Analytical error for Mg/Ca (0.1 mmol/mol) is equivalent to the height of the symbols.

phase with peak summer BWT (Scourse et al., 2004), i.e. September for the Arctic Ocean. Another study based in Kongsfjorden (Svalbard) found interspecies variability; one species calcified in summer, another appeared to have

continuous reproduction/growth lasting from July to November, while *N. labradorica*, also investigated in this study, calcified in autumn (Skirbekk et al., 2016). Understanding the seasonal nature of Mg/Ca-BWT signals is

clearly important for developing and interpreting palaeotemperature proxies.

4.2. Integration of Arctic benthic foraminifera Mg/Ca-BWT data with existing records

A further step in analyzing the Arctic Ocean Mg/Ca data is to compare it to existing monospecific compilations of benthic Mg/Ca data from wider temperature ranges and different ocean basins. By combining published data (thoroughly cleaned, or adjusted to cleaned values, see methods), we see how the Arctic benthic foraminifera Mg/Ca data provide important new constraints at low temperatures for six species, including several covered only sparsely in previous studies and one common species for which no published data exist (*E. clavatum*) (Fig. 8). For the five species where previous data are available (Appendix Table C shows the origin of each dataset), we provide revised linear and exponential regressions that include our new constraints (Table 3). We note that care should be taken when compiling epifaunal benthic foraminifera Mg/Ca global datasets if the bottom waters from the sites experience low $\Delta[\text{CO}_3^{2-}]$ because Mg/Ca values may mainly reflect $\Delta[\text{CO}_3^{2-}]$ changes instead of BWT (Elderfield et al., 2006). Therefore, in the presented *C. wuellerstorfi* compilation we have not included undersaturated data from deep sites found in Russell et al. (1994), Martin et al. (2002), Healey et al. (2008), Raitzsch et al. (2008), and Yu and Elderfield (2008) studies.

For the genus *Elphidium*, no previous calibrations were found to date. The regression presented here, therefore, is based on the Arctic *E. clavatum* dataset alone (Fig. 8a).

While we have no other comparison, the infaunal habitat and absence of any relationship between Mg/Ca and $\Delta[\text{CO}_3^{2-}]$ gives confidence that this species should make a suitable palaeothermometry tracer. We present a Mg/Ca-BWT linear sensitivity of $0.125 \text{ mmol/mol/}^\circ\text{C}$ ($\text{Mg/Ca} = 0.816 \pm 0.06 + 0.125 \pm 0.05 \times \text{BWT}$, $r^2 = 0.4$), which is realistic considering benthic foraminifera sensitivity found in several previous studies using different species (Lear et al., 2002; Marchitto et al., 2007; Lear et al., 2010; Tisserand et al., 2013). Our *N. labradorica* and *C. neoteretis* Mg/Ca data, both also infaunal, fit previous published trends (Fig. 8b and c). *Nonionella labradorica* is a common species of Arctic shelf waters. Combining the Arctic *N. labradorica* data with that from Kongsfjorden, Svalbard (Skirbekk et al., 2016; Fig. 8b) expands the cold end of the field dataset by 3°C , and can be described by the relationship: $\text{Mg/Ca} = 1.325 \pm 0.01 \times e^{(0.065 \pm 0.01 \times \text{BWT})}$, $r^2 = 0.9$. The resulting revised linear sensitivity is $0.090 \text{ mmol/mol/}^\circ\text{C}$, that is very close, i.e. within error, to Skirbekk et al.'s (2016) original (autumn only) linear fit ($0.088 \text{ mmol/mol/}^\circ\text{C}$). A reason for this consistency could be the infaunal habitat, that minimizes any potential complications due to low bottom water $\Delta[\text{CO}_3^{2-}]$. This is encouraging and suggests *N. labradorica* could be a useful Mg/Ca signal carrier in shelf settings. *Cassidulina neoteretis* is the most common species in the Arctic Ocean Atlantic layer and is also common throughout North Atlantic, Nordic and Arctic shelf settings (Seidenkrantz, 1995; Lazar et al., 2016). We find a robust fit when we combine the new Arctic data with data from the northern Icelandic shelf (Kristjánsdóttir et al., 2007); there is a small overlap between the two datasets (Fig. 8c, Table 3) and the new data extend the cold end from 0.22°C to

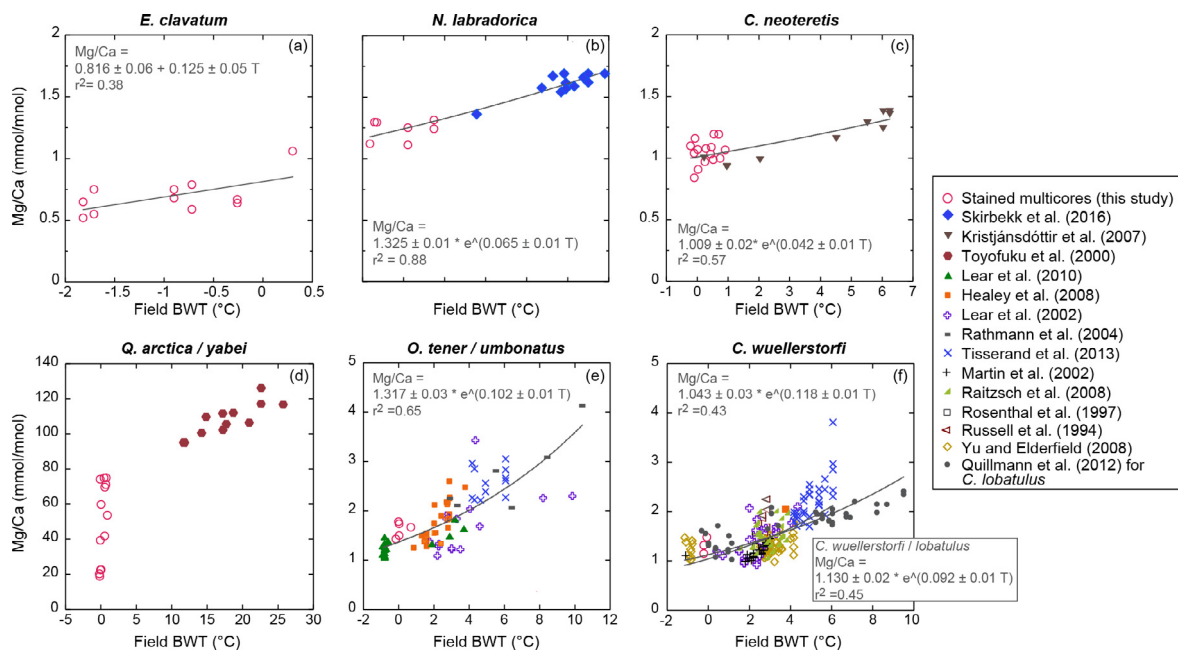


Fig. 8. Arctic benthic foraminiferal trace metal data for the six species investigated in this study compared to published data derived from the Atlantic, Pacific and Indian Oceans for the same taxa. The Mg/Ca and field BWT axes scales are customized per species reflecting the different test Mg concentrations typifying individual taxa. New exponential fits to the monospecific compilations are shown (equations in the figures), apart from *E. clavatum* (a) for which no existing data was found. In this case a linear fit is preferred because of the narrow temperature range of the Arctic-only constraints. Curve fits were not applied to the compiled *Q. arctica / yabei* dataset.

−0.47 °C in this species. This leads to an exponential fit of $Mg/Ca = 1.009 \pm 0.02 \times e^{(0.042 \pm 0.01 \times BWT)}$, $r^2 = 0.6$. We suggest this might be an option for capturing low temperature variations in the Atlantic sourced waters in the Arctic Ocean.

We see somewhat different patterns for the three epifaunal species investigated. The porcelaneous species *Q. arctica* shows a strikingly larger Mg/Ca range for minimal temperature change compared to both other Arctic species and the only other published dataset for *Quinqueloculina*, which comes from a culture study of the species *Q. yabei*, common in tidal pools off the coast of Japan (Toyofuku et al., 2000) (Fig. 8d). This result implies that, for this taxon, different factors control Mg/Ca in different locations. Specifically, this suggests that under the low temperatures of the Arctic Ocean, $\Delta[CO_3^{2-}]$ has a stronger influence on *Q. arctica* Mg/Ca than temperature (Fig. 7d) (see Section 4.3 for further discussion).

Oridorsalis tener was found at sites bathed by Atlantic water and Arctic deep waters. This species may be considered the polar variant of *O. umbonatus* (Wollenburg and Mackensen, 1998a; Wollenburg et al., 2007), which has proved useful for Mg/Ca BWT reconstructions in a number of other calibration studies (Lear et al., 2002, 2010; Martin et al., 2002; Rathmann et al., 2004; Healey et al., 2008) and it is a preferred Mg/Ca signal carrier in early Cenozoic palaeoclimate reconstructions. Therefore, we compared the Arctic *O. tener* Mg/Ca with various published datasets for *O. umbonatus*. The resulting Mg/Ca data compilation fits reasonably well with existing correlations (Fig. 8e). However, we notice that our few Arctic data points all sit slightly above the regression curve. While this could be within sample/method error, it is possible that this is a consequence of differences in their depth habitat, epifaunal for *O. tener*, shallow infaunal for *O. umbonatus*. Alternatively, the *O. tener/umbonatus* mismatch may derive from authigenic Mg-enrichment in the material collected from Little Bahama Bank, as suggested by the authors (Lear et al., 2002). This observation highlights the point that integrating data to build single-species Mg/Ca-BWT relationships is likely to add additional noise, since each setting has its own unique oceanic and taphonomic characteristics that could overprint the temperature signals. An additional consideration for this larger *O. umbonatus* dataset is the use of different test size windows between the studies that could represent another variable that can introduce noise due to potential metabolic or ontogenetic effects that alter the quantities of Mg entering the calcite. For example, Tisserand et al. (2013) showed that *O. umbonatus* from a 250 to 400 μm size window had Mg/Ca values ~ 0.4 mmol/mol Mg/Ca lower compared to tests in the 150–250 μm size range. This size consideration could be relevant to our Arctic *O. tener* since it is smaller (125–250 μm) and thinner-walled than the compiled *O. umbonatus* data (250–400 μm). The slightly higher Mg/Ca in our Arctic data (Fig. 8e), thus, may be the result of ontogenetic vital effects (Lear, 2000; Elderfield et al., 2002). Despite these considerations, *O. tener* might be useful for tracing relative BWT changes in deeper water Arctic settings and the refined calibration results in $Mg/Ca = 1.317 \pm 0.03 \times e^{(0.102 \pm 0.01 BWT)}$, $r^2 = 0.7$.

Cibicidoides wuellerstorfi is the most widely investigated species for Mg/Ca palaeothermometry (Rosenthal et al., 1997; Lear et al., 2002, 2010; Martin et al., 2002; Elderfield et al., 2006; Healey et al., 2008; Raitzsch et al., 2008; Tisserand et al., 2013). The Arctic data for this species are too few to make any meaningful regional calibration. Therefore, we combine it with published core-top data, exclusively for *C. wuellerstorfi*, from sites above the hypothesized threshold for significant Mg interference with $\Delta[CO_3^{2-}]$ (30 $\mu mol/kg$) (Elderfield et al., 2006; Marchitto et al., 2007; Yu and Elderfield, 2008). This new “well-saturated” compilation (Fig. 8f, Table 3) can be described by the exponential equation $Mg/Ca = 1.043 \pm 0.03 \times e^{(0.118 \pm 0.1 BWT)}$, $r^2 = 0.4$. Although the r^2 value is weaker than previous studies, the temperature sensitivity is consistent with previous studies (Lear et al., 2002; Martin et al., 2002; Raitzsch et al., 2008) supporting the use of this species for Mg/Ca-palaeothermometry. For additional comparison we have integrated the cold water North Atlantic *C. lobatulus* Mg/Ca dataset from Quillmann et al. (2012) that expands the calibration by ~ 2 °C at the warmest end (Fig. 8f). The *C. lobatulus* data show consistencies with the compiled *C. wuellerstorfi* data at the < 4 °C cold end. However, at > 5 °C the *C. lobatulus* Mg/Ca values are lower by ~ 1 mmol/mol and less scattered than the values for *C. wuellerstorfi* from Tisserand et al. (2013) at similar temperatures.

In summary, inclusion of the new Arctic Ocean data modifies the global regression curves for different species of benthic foraminifera. The revised regressions appear to work best for infaunal taxa. They produce relationships that are broadly consistent with previous findings, although in all cases lowering the Mg/Ca-BWT sensitivity (Table 3) possibly caused by the addition of Mg/Ca values at the coldest part of the exponential relationship.

4.3. $\Delta[CO_3^{2-}]$ effect

Temperature typically has the strongest control on Mg incorporation into benthic foraminifera calcite. However, as discussed above, it has been shown that $\Delta[CO_3^{2-}]$ can have a significant influence when temperatures are below 3 °C and $\Delta[CO_3^{2-}] < 30 \mu mol/kg$ (Martin et al., 2002; Elderfield et al., 2006; Marchitto et al., 2007; Yu and Elderfield, 2008). This effect had not previously been systematically studied in Arctic Ocean benthic foraminifera.

Given that Arctic bottom waters are all colder than 3 °C and $\Delta[CO_3^{2-}]$ ranges between -10 and $55 \mu mol/kg$, we might expect some influence of $\Delta[CO_3^{2-}]$ on benthic Mg/Ca, especially in the halocline sites experiencing the lowest $\Delta[CO_3^{2-}]$ and BWT (Fig. 3). It has been suggested that bottom water $\Delta[CO_3^{2-}]$ influences pore water $\Delta[CO_3^{2-}]$ (Weldeab et al., 2016), however we see no systematic relationship between bottom water $\Delta[CO_3^{2-}]$ and test Mg/Ca in any of the infaunal stained hyaline species (Fig. 7). For *E. clavatum* and *N. labradorica*, common at the halocline stations, the lack of influence of bottom water $\Delta[CO_3^{2-}]$ on test Mg/Ca might be a consequence of their infaunal habitat where test calcification takes place using buffered pore waters. Similar ideas have been proposed to explain

infaunal vs. epifaunal foraminifera Mg/Ca response with respect to early Cenozoic palaeoclimate events where extremes of $\Delta[\text{CO}_3^{2-}]$ are thought to have occurred (Katz, 2003; Elderfield et al., 2010; Lear et al., 2015). We conclude, therefore, that for the infaunal hyaline species studied here, bottom water $\Delta[\text{CO}_3^{2-}]$ is not the major control on test Mg/Ca at the coldest BWT prevailing in the Arctic, nor an obvious source of error complicating our Mg/Ca-BWT investigations. This is not the case for high-Mg calcite porcelaneous species *Q. arctica*, which shows a strong correlation between Mg/Ca and $\Delta[\text{CO}_3^{2-}]$. The small sample size for *O. tener* and *C. wuellerstorfi* preclude further evaluation of any $\Delta[\text{CO}_3^{2-}]$ effect in hyaline epifaunal benthic foraminifera, although the bottom water $\Delta[\text{CO}_3^{2-}]$ were above the 30 $\mu\text{mol/kg}$ threshold.

4.3.1. Mg/Ca and calcification in *Quinqueloculina arctica*

The high Mg calcite tests of *Q. arctica* display a higher linear correlation between Mg/Ca and $\Delta[\text{CO}_3^{2-}]$ ($r^2 = 0.77$, $n = 13$) than between Mg/Ca and BWT ($r^2 = 0.37$, $n = 13$) (Figs. 7d and 6d). This implies that temperature is not the dominant control on Mg partitioning into *Q. arctica* at the cold bottom waters of the Arctic Ocean. This is in line with the low temperature control found in other porcelaneous species when compared to hyaline species (Pawlowski et al., 2003; de Nooijer et al., 2009). *Quinqueloculina arctica* is regarded as having an epifaunal habitat, thus directly exposed to bottom waters. In general, the bottom water saturation state decreases with increasing water depth for these core-tops, with the decreasing $\Delta[\text{CO}_3^{2-}]$ driven by the pressure related increase in $[\text{CO}_3^{2-}]_{\text{SAT}}$ (Table 2). However, there is a clear outlier with low $\Delta[\text{CO}_3^{2-}]$ at shallow water depths (Fig. 7d). This station (SW-L2-21-MC) is the shallowest site on the Eastern Siberian slope and is known to be strongly influenced by Pacific waters (Anderson et al., 2016). Despite the low bottom water $\Delta[\text{CO}_3^{2-}]$ of this site, the *Q. arctica* Mg/Ca is relatively high (Fig. 7d). We believe this outlier is not an analytical error since *Q. arctica* B/Ca and Sr/Ca ratios are also offset from the rest of the data. We think that the low $\Delta[\text{CO}_3^{2-}]$ of this shallow site is driven by the high DIC content of the Pacific influenced waters. Recent foraminiferal culture experiments show that when seawater CO_2 is increased, diffusion of CO_2 into foraminiferal protoplasm and its conversion into CO_3^{2-} using H_2O promotes calcification (Toyofuku et al., 2017). At the same time intra cell Ca^{2+} transport must decrease to regulate the degree of Ca saturation for calcite causing trace element increases in the final precipitated calcite (Keul et al., 2016). Without drawing too many conclusions on the basis of a single core-top analysis, we suggest that paired trace metal analyses of high-Mg calcite and low-Mg calcite foraminifera have the potential to provide useful constraints on carbonate system parameters.

5. CONCLUSIONS

The application of benthic foraminifera Mg/Ca palaeothermometry in the cold bottom waters of the Arctic Ocean was investigated. An initial survey of Arctic benthic foraminifera Mg/Ca, a region where these data are espe-

cially scarce, identified six species that were abundant enough to collectively sample the three main water masses resident in the Arctic Ocean; i.e. the halocline (*E. clavatum*, *N. labradorica*); Atlantic water (mainly *C. neoteretis*, *Q. arctica*) and Arctic deep water (mainly *C. wuellerstorfi* and *O. tener*). Our Mg/Ca data obtained from the five studied hyaline species ranged from 0.5 mmol/mol in *E. clavatum* to 1.8 mmol/mol in *O. tener*, whereas distinct mineralogical tests of porcelaneous *Q. arctica* varied between 18 and 75 mmol/mol.

The new Arctic benthic foraminifera Mg/Ca data provide valuable new constraints at the coldest end ($<1^\circ\text{C}$) of the BWT spectrum. By adding our Arctic Ocean results to existing datasets we have significantly improved the calibrations for the five hyaline widespread taxa studied here across the -1 to $+10^\circ\text{C}$ range. Notably, the hyaline taxa have low Mg/Ca ratios at low temperatures consistent with theory and empirical evidence, broadly fitting with previous studies. The three infaunal species *E. clavatum*, *N. labradorica*, and *C. neoteretis* showed the greatest correspondence between test Mg/Ca and temperature. This is an important finding and encouraging with respect to using Arctic infaunal benthic foraminifera Mg/Ca-palaeothermometry in Arctic and subarctic regions. The calculated sensitivities for epifaunal species *C. wuellerstorfi* and *O. tener* rely on less datapoints but are largely consistent with previous findings. Specially, *O. tener* show slightly higher Mg/Ca values compared to the predicted linear or exponential fits derived from data outside the Arctic. We attribute this offset to a test size effect in *O. tener* as it grows smaller and has a shallower habitat in the Arctic than in other oceans.

The $\Delta[\text{CO}_3^{2-}]$ -BWT relationship observed in this Arctic study supports the idea that there is a threshold value in $\Delta[\text{CO}_3^{2-}]$ of 30 $\mu\text{mol/kg}$ below which $\Delta[\text{CO}_3^{2-}]$ may have a stronger effect than temperature on Mg incorporation into test calcite. However, none of the hyaline species investigated showed Mg/Ca- $\Delta[\text{CO}_3^{2-}]$ relationships, even when measured bottom water $\Delta[\text{CO}_3^{2-}]$ was low and potentially corrosive to biogenic calcite (i.e. below $\Delta[\text{CO}_3^{2-}]$ of 30 $\mu\text{mol/kg}$). In contrast, the porcelaneous (high Mg calcite) epifaunal taxon *Q. arctica* behaves differently, and appears to be highly sensitive to bottom water $\Delta[\text{CO}_3^{2-}]$. This species, therefore, is not appropriate for tracing temperature in the Arctic Ocean.

ACKNOWLEDGEMENTS

The authors are grateful to I/B Oden scientific and crew party during Expedition SWERUS-C3 for their help in the logistics during water and sediment sampling. Anne Jennings for kindly providing a stained foraminifera sample from Petermann-2015 Expedition. We thank E. Mawbey and A. Morte-Ródenas for teaching sample cleaning and ICP-MS operation. This study forms a part of the SWERUS-C3 program (Swedish-Russian-US Arctic Ocean Investigation of Climate-Cryosphere-Carbon Interactions). This research was supported by the Knut and Alice Wallenberg Foundation, Swedish Polar Research Secretariat, Stockholm University and the Swedish Research Council (VR).

APPENDIX A. SUPPLEMENTARY MATERIAL

Supplementary data associated with this article can be found, in the online version, at <https://doi.org/10.1016/j.gca.2018.02.036>.

REFERENCES

- Altenbach A. V. and Sarnthein M. (1989) Productivity record in benthic foraminifera. In *Productivity of the Ocean: Present and Past* (eds. W. H. Berger, V. S. Smetacek and G. Wefer). John Wiley, Chichester, pp. 255–269.
- Anderson L. G., Björk G., Holby O., Jutterström S., Mörth C. M., Regan M. O., Pearce C., Semiletov I., Stranne C., Stöven T. and Tanhua T. (2016) Shelf-basin interaction along the Laptev-East Siberian Seas. *Ocean Sci. Discuss.*, 1–26.
- Astakhov A. S., Bosin A. A., Kolesnik A. N. and Obrezkova M. S. (2015) Sediment geochemistry and diatom distribution in the Chukchi sea: application for bioproductivity and paleoceanography. *Oceanography* **28**, 190–201.
- Barker S., Greaves M. and Elderfield H. (2003) A study of cleaning procedures used for foraminiferal Mg/Ca paleothermometry. *Geochemistry. Geophys. Geosyst.* **4**, 1–20.
- Bergsten H. (1994) Recent benthic foraminifera of a transect from the North-Pole to the Yermak Plateau, eastern Central Arctic Ocean. *Mar. Geol.* **119**, 251–267.
- Billups K. and Schrag D. P. (2002) Paleotemperatures and ice volume of the past 27 Myr revisited with paired Mg/Ca and $^{18}\text{O}/^{16}\text{O}$ measurements on benthic foraminifera. *Paleoceanography* **17**, 1003.
- Boltovskoy E. and Wright R. (1976) Recent Foraminifera. Springer Netherlands. p. 515. [10.1007/978-94-017-2860-7](https://doi.org/10.1007/978-94-017-2860-7).
- Boyle E. A. (1983) Manganese carbonate overgrowths on foraminifera tests. *Geochim. Cosmochim. Acta* **47**, 1815–1819.
- Boyle E. A. and Keigwin L. D. (1985) Comparison of Atlantic and Pacific paleochemical records for the last 215,000 years: changes in deep ocean circulation and chemical inventories. *Earth Planet. Sci. Lett.* **76**, 135–150.
- Broecker W. and Peng T. (1992) Interhemispheric transport of carbon dioxide by ocean circulation. *Nature* **356**, 587–589.
- Carmack E. C., Macdonald R. W., Perkin R. G., McLaughlin F. A. and Pearson R. J. (1995) Evidence for warming of Atlantic water in the Southern Canadian Basin of the Arctic Ocean: results from the Larsen-93 Expedition. *Geophys. Res. Lett.* **22**, 1061–1064.
- Chierici M. and Fransson A. (2009) Calcium carbonate saturation in the surface water of the Arctic Ocean: undersaturation in freshwater influenced shelves. *Biogeosci. Discuss.* **6**, 4963–4991.
- Corliss B. H. and Emerson S. (1990) Distribution of rose bengal stained deep-sea benthic foraminifera from the Nova Scotian continental margin and Gulf of Maine. *Deep Sea Res. Part A Oceanogr. Res. Pap.* **37**, 381–400.
- Corliss B. and Silva K. A. (1993) Rapid growth of deep-sea benthic foraminifera. *Geology* **21**, 991–994.
- Cronin T. M., Dwyer G. S., Farmer J., Bauch H. a., Spielhagen R. F., Jakobsson M., Nilsson J., Briggs W. M. and Stepanova A. (2012) Deep Arctic Ocean warming during the last glacial cycle. *Nat. Geosci.* **5**, 631–634.
- Dabbous S. A. and Scott D. B. (2012) Short-term monitoring of Halifax Harbour (Nova Scotia, Canada) pollution remediation using benthonic foraminifera as proxies. *J. Foraminifer. Res.* **42**, 187–205.
- Debenay J.-P., Pawłowski J. and Decrouez D. (1996) *Les foraminifères actuels*. Masson, Paris Milan Barcelone.
- Dickson A. G. and Millero F. J. (1987) A comparison of the equilibrium constants for the dissociation of carbonic acid in seawater media. *Deep Sea Res. Part A Oceanogr. Res. Pap.* **34**, 1733–1743.
- Dissard D., Nehrke G., Reichart G. J. and Bijma J. (2010) The impact of salinity on the Mg/Ca and Sr/Ca ratio in the benthic foraminifera *Ammonia tepida*: results from culture experiments. *Geochim. Cosmochim. Acta* **74**, 928–940.
- Dmitrenko I. A., Kirillov S. A., Ivanov V. V., Woodgate R. A., Polyakov I. V., Koldunov N., Louis Fortier L., Lalonde C., Kaleschke L., Bauch D., Hölemann J. A. and Timokhov L. A. (2009) Seasonal modification of the Arctic Ocean intermediate water layer off the eastern Laptev Sea continental shelf break. *J. Geophys. Res.* **114**, C06010. <https://doi.org/10.1029/2008JC005229>.
- Elderfield H., Vautravers M. and Cooper M. (2002) The relationship between shell size and Mg/Ca, Sr/Ca, $\delta^{18}\text{O}$, and $\delta^{13}\text{C}$ of species of planktonic foraminifera. *Geochem. Geophys. Geosyst.* **3**, 1–13.
- Elderfield H., Yu J., Anand P., Kiefer T. and Nyland B. (2006) Calibrations for benthic foraminiferal Mg/Ca paleothermometry and the carbonate ion hypothesis. *Earth Planet. Sci. Lett.* **250**, 633–649.
- Elderfield H., Greaves M., Barker S., Hall I. R., Tripathi A., Ferretti P., Crowhurst S., Booth L. and Daunt C. (2010) A record of bottom water temperature and seawater $\delta^{18}\text{O}$ for the Southern Ocean over the past 440 kyr based on Mg/Ca of benthic foraminiferal *Uvigerina* spp. *Quat. Sci. Rev.* **29**, 160–169.
- Farmer J. R., Cronin T. M., De Vernal A., Dwyer G. S., Keigwin L. D. and Thunell R. C. (2011) Western Arctic Ocean temperature variability during the last 8000 years. *Geophys. Res. Lett.* **38**, 1–6.
- Farmer J. R., Cronin T. M. and Dwyer G. S. (2012) Ostracode Mg/Ca paleothermometry in the North Atlantic and Arctic oceans: evaluation of a carbonate ion effect. *Paleoceanography* **27**, 1–14.
- Green K. E. (1960) Ecology of some Arctic foraminifera. *Micropaleontology* **6**(1), 57–78.
- Gustafsson M. and Nordberg K. (1999) Benthic foraminifera and their response to hydrography, periodic hypoxic conditions and primary production in the Koljo fjord on the Swedish west coast. *J. Sea Res.* **41**, 163–178.
- Gustafsson M. and Nordberg K. (2001) Living (Stained) Benthic foraminiferal response to primary production and hydrography in the deepest part of the Gullmar Fjord, Swedish West Coast, with comparisons to Høglund's 1927 material. *J. Foraminifer. Res.* **31**, 2–11.
- Healey S. L., Thunell R. C. and Corliss B. H. (2008) The Mg/Ca-temperature relationship of benthic foraminiferal calcite: new core-top calibrations in the <math> < 4\text{ }^\circ\text{C}</math> temperature range. *Earth Planet. Sci. Lett.* **272**, 523–530.
- Jutterström S. and Anderson L. G. (2005) The saturation of calcite and aragonite in the Arctic Ocean. *Mar. Chem.* **94**, 101–110.
- Katz M. E. (2003) Early Cenozoic benthic foraminiferal isotopes: species reliability and interspecies correction factors. *Paleoceanography* **18**, 1–12.
- Keul N., Langer G., Thoms S., Jan de Nooijer L., Reichart G.-J. and Bijma J. (2016) Exploring foraminiferal Sr/Ca as a new carbonate system proxy. *Geochim. Cosmochim. Acta* **202**, 374–386.
- Kristjánsdóttir G. B., Lea D. W., Jennings A. E., Pak D. K. and Belanger C. (2007) New spatial Mg/Ca-temperature calibrations for three Arctic, benthic foraminifera and reconstruction of north Iceland shelf temperature for the past 4000 years. *Geochem., Geophys. Geosyst.* **8**, Q03P21.
- Lagoe M. B. (1977) Recent benthic Foraminifera from the central Arctic Ocean. *J. Foraminifer. Res.* **7**, 106–129.

- Lazar K. B., Polyak L. and Dipre G. R. (2016) Re-examination of the use of *Cassidulina neoteretis* as a Pleistocene biostratigraphic marker in the Arctic Ocean. *J. Foraminifera Res.* **46**, 115–123.
- Lear C. H. (2000) Evolution of Cenozoic Ocean Composition and Temperature from Foraminiferal Trace Element Proxies. University of Cambridge.
- Lear C. H., Elderfield H. and Wilson P. A. (2000) Cenozoic deep-sea temperatures and global ice volumes from Mg/Ca in benthic foraminiferal calcite. *Science* **287**, 269–272.
- Lear C. H., Rosenthal Y. and Slowey N. (2002) Benthic foraminiferal Mg/Ca-paleothermometry: a revised core-top calibration. *Geochim. Cosmochim. Acta* **66**, 3375–3387.
- Lear C. H., Mawbey E. M. and Rosenthal Y. (2010) Cenozoic benthic foraminiferal Mg/Ca and Li/Ca records: toward unlocking temperatures and saturation states. *Paleoceanography* **25**, 1–11.
- Lear C. H., Coxall H. K., Foster G. L., Lunt D. J., Mawbey E. M., Rosenthal Y., Sosdian S. M., Thomas E. and Wilson P. A. (2015) Neogene ice volume and ocean temperatures: insights from infaunal foraminiferal Mg/Ca paleothermometry. *Paleoceanography* **30**, 1437–1454.
- Locarnini, R. A., Mishonov, A.V., Antonov, J.I., Boyer, T.P., Garcia, H.E., Baranova, O.K., Zweng, M.M., Paver, C.R., Reagan, J.R., Johnson, D.R., Hamilton, M. and Seidov, D., (2013) World Ocean Atlas 2013, Volume 1: Temperature. S. Levitus, Ed., A. Mishonov Technical Ed.; NOAA Atlas NESDIS 73, 40.
- Luchin V. and Panteleev G. (2014) Deep-sea research II thermal regimes in the Chukchi Sea from 1941 to 2008. *Deep. Res. Part II* **109**, 14–26.
- Marchitto T. M., Bryan S. P., Curry W. B. and McCorkle D. C. (2007) Mg/Ca temperature calibration for the benthic foraminifer *Cibicidoides pachyderma*. *Paleoceanography* **22**, 1–9.
- Martin P. A., Lea D. W., Rosenthal Y., Shackleton N. J., Sarnthein M. and Papenfuss T. (2002) Quaternary deep sea temperature histories derived from benthic foraminiferal Mg/Ca. *Earth Planet. Sci. Lett.* **198**, 193–209.
- Mehrbach C., Culbertson C. H., Hawley J. E. and Pytkowicz R. M. (1973) Measurement of the apparent dissociation constants of carbonic acid in seawater at atmospheric pressure. *Limnol. Oceanogr.* **18**, 897–907.
- Münchow A. and Heuzé C. (2015) CTD Rosette Operations on I/B Oden's Petermann-2015 Expedition.
- Murray J. W. (2006) *Ecology and Applications of Benthic Foraminifera*. Cambridge University Press.
- Myers E. H. (1938) The present state of our knowledge concerning the life cycle of the foraminifera. *Proc. Natl. Acad. Sci. USA* **24**, 10–17.
- de Nooijer L. J., Toyofuku T. and Kitazato H. (2009) Foraminifera promote calcification by elevating their intracellular pH. *Proc. Natl. Acad. Sci.* **106**, 15374–15378.
- Osterman L. E., Poore R. Z. and Foley K. M. (1999) Distribution of benthic foraminifera (>125 µm) in the surface sediments of the Arctic Ocean. *United States Geol. Surv. Bull.* **2164**, 28.
- Pawlowski J., Holzmann M., Berney C., Fahrni J., Gooday A. J., Cedhagen T., Habura A. and Bowser S. S. (2003) The evolution of early Foraminifera. *Proc. Natl. Acad. Sci.* **100**, 11494–11498.
- Pisareva M. N., Pickart R. S., Iken K., Ershova E. A., Grebmeier J. M., Cooper L. W., Bluhm B. A., Nobre C., Hopcroft R. R., Hu H., Wang J., Ashjian C. J., Kosobokova K. N. and Whitley T. E. (2015) The relationship between patterns of benthic fauna and zooplankton in the Chukchi Sea and physical forcing. *Oceanography* **28**, 68–83.
- Polyakov I. V., Beszczynska A., Carmack E. C., Dmitrenko I. A., Fahrbach E., Frolov I. E., Gerdes R., Hansen E., Holfort J., Ivanov K. A., Johnson M. A., Karcher M., Kauker F., Morison J., Orvik K. A., Schauer U., Simmons H. L., Skagseth Ø., Sokolov V. T., Steele M., Timokhov L. A., Walsh D. and Walsh J. E. (2005) One more step toward a warmer Arctic. *Geophys. Res. Lett.* **32**, 1–4.
- Polyakov I. V., Walsh J. E. and Kwok R. (2012) Recent changes of Arctic multiyear sea ice coverage and the likely causes. *Bull. Am. Meteorol. Soc.* **93**, 145–151.
- Quadfasel D., Sy A., Wells D. and Tunik A. (1991) Warming in the Arctic. *Nature* **350**, 385.
- Quillmann U., Marchitto T., Jennings A., Andrews J. T. and Friestad B. F. (2012) Cooling and freshening at 8.2 ka on the NW Iceland Shelf recorded in paired δ18O and Mg/Ca measurements of the benthic foraminifer *Cibicides lobatulus*. *Quat. Res.* **78**, 528–539.
- Raitzsch M., Kuhnert H., Groeneveld J. and Bickert T. (2008) Benthic foraminifer Mg/Ca anomalies in South Atlantic core top sediments and their implications for paleothermometry. *Geochem., Geophys. Geosyst.* **9**.
- Rathmann S., Hess S., Kuhnert H. and Mulitza S. (2004) Mg/Ca ratios of the benthic foraminifera *Oridorsalis umbonatus* obtained by laser ablation from core top sediments: Relationship to bottom water temperature. *Geochem. Geophys. Geosyst.* **5**, 1–10.
- Rathburn A. E. and De Deckker P. (1997) Magnesium and strontium compositions of Recent benthic foraminifera from the Coral Sea, Australia and Prydz Bay, Antarctica. *Mar. Micropaleontol.* **32**, 231–248.
- Ries J. B. (2010) Review: geological and experimental evidence for secular variation in seawater Mg/Ca (calcite-aragonite seas) and its effects on marine biological calcification. *Biogeosciences* **7**, 2795–2849.
- Robbins L. L., Hansen M. E., Kleypas J. A. and Meylan S. C. (2010) CO2calc – a user-friendly seawater carbon calculator for Windows, Mac OS X and iOS (iPhone). U.S. Geol. Surv. Open-File Rep. 2010–1280, 17.
- Rosenthal Y., Boyle E. and Slowey N. (1997) Environmental controls on the incorporation of magnesium, strontium, fluorine and cadmium into benthic foraminiferal shells from little bahama bank: prospects for thermocline paleoceanography. *Geochim. Cosmochim. Acta* **61**, 3633–3643.
- Rosenthal Y., Field M. P. and Sherrell R. M. (1999) Precise determination of element/calcium ratios in calcareous samples using sector field inductively coupled plasma mass spectrometry. *Anal. Chem.* **71**, 3248–3253.
- Rosenthal Y., Lear C. H., Oppo D. W. and Linsley B. K. (2006) Temperature and carbonate ion effects on Mg/Ca and Sr/Ca ratios in benthic foraminifera: aragonitic species *Hoeglundina elegans*. *Paleoceanography* **21**, 1–14.
- Rudels B., Jones E. P., Anderson L. G. and Kattner G. (1994) On the intermediate depth waters of the Arctic Ocean. Polar Ocean. their role Shap. *Glob. Environ.*, 525.
- Rudels B. (2009) Arctic ocean circulation. *Encyclopedia of Ocean Sci.*, 211–225. <https://doi.org/10.1016/B978-012374473-9.00601-9>.
- Rudels B., Anderson L., Eriksson P., Fahrbach E., Jakobsson M., Jones E. P., Melling H., Prinsenberg S., Schauer U. and Yao T. (2012) Observations in the ocean. In *Arctic Climate Change: The ACSYS decade and beyond* (eds. P. Lemke and H. -W. Jacobi). Springer. pp. 117–198.
- Russell A. D., Emerson S., Nelson B. K., Erez J. and Lea D. W. (1994) Uranium in foraminiferal calcite as a recorder of seawater uranium concentrations. *Geochim. Cosmochim. Acta* **58**, 671–681.
- Schafer C. T., Wagner F. J. E. and Ferguson C. (1975) Occurrence of foraminifera, molluscs and ostracods adjacent to the

- industrialized shoreline of Canso Strait, Nova Scotia. *Water Air Soil Pollut.* **5**, 79–96.
- Schauer U., Beszczynska-Möller A., Walczowski W., Fahrbach E., Piechura J. and Hansen E. (2008) Variation of measured heat flow through the Fram Strait between 1997 and 2006. Arctic-Subarctic Ocean Fluxes Defin. role North. Seas Clim. 65–85.
- Schauer U., Fahrbach E., Osterhus S. and Rohardt G. (2004) Arctic warming through the Fram Strait: Oceanic heat transport from 3 years of measurements. *J. Geophys. Res. C Ocean.* **109**, 1–14.
- Schönfeld J., Alve E., Geslin E., Jorissen F., Korsun S., Spezzaferri S., Abramovich S., Almogi-Labin A., du Chatelet E. A., Barras C., Bergamin L., Bicchi E., Bouchet V., Cearreta A., Di Bella L., Dijkstra N., Disaro S. T., Ferraro L., Frontalini F., Gennari G., Golikova E., Haynert K., Hess S., Husum K., Martins V., McGann M., Oron S., Romano E., Sousa S. M. and Tsujimoto A. (2012) The FOBIMO (FOraminiferal BLO-MONitoring) initiative-Towards a standardised protocol for soft-bottom benthic foraminiferal monitoring studies. *Mar. Micropaleontol.* **94–95**, 1–13.
- Scott D. B., Mudie P. J., Vernal A., De Baki V., Mackinnon K. D., Medioli F. S. and Mayer L. (1989) *Lithostratigraphy, Biostratigraphy, and Stable-Isotope Stratigraphy of Cores From ODP Leg 105 Site Surveys*. Labrador Sea and Baffin Bay, IODP, p. 105.
- Scott D. B. and Vilks G. (1991) Benthic foraminifera in the surface sediments of the deep-sea Arctic Ocean. *J. Foraminifer. Res.* **21**, 20–38.
- Scott D. B., Schell T., Rochon a and Blasco S. (2008) Modern benthic foraminifera in the surface sediments of the Beaufort Shelf, Slope and Mackenzie Trough, Beaufort Sea, Canada: taxonomy and summary of surficial distributions. *J. Foraminifer. Res.* **38**, 228–250.
- Scourse J., Kennedy H., Scott G. and Austin W. (2004) Stable isotopic analyses of modern benthic foraminifera from seasonally stratified shelf seas: disequilibria and the 'seasonal effect'. *The Holocene* **14**, 747–758.
- Seidenkrantz M.-S. (1995) *Cassidulina teretis* Tappan and *Cassidulina neoteretis* new species (Foraminifera): stratigraphic markers for deep sea and outer shelf areas. *J. Micropaleontol.* **14**, 145–157.
- Serreze M. C. and Barry R. G. (2011) Processes and impacts of Arctic amplification: a research synthesis. *Glob. Planet. Change* **77**, 85–96.
- Skirbekk K., Hald M., Marchitto T. M., Junttila J., Klitgaard Kristensen D. and Aagaard Sørensen S. (2016) Benthic foraminiferal growth seasons implied from Mg/Ca-temperature correlations for three Arctic species. *Geochem. Geophys. Geosyst.* **17**, 1–21.
- Stanley S. M. and Hardie L. A. (1999) Hypercalcification: paleontology links plate tectonics and geochemistry to sedimentology. *GSA Today* **9**, 1–7.
- Steele M. and Boyd T. (1998) Retreat of the cold halocline layer in the Arctic Ocean. *J. Geophys. Res.* **103**, 10419–10435.
- Tisserand A. A., Dokken T. M., Waelbroeck C., Gherardi J. M., Scao V., Fontanier C. and Jorissen F. (2013) Refining benthic foraminiferal Mg/Ca-temperature calibrations using core-tops from the western tropical Atlantic: implication for paleotemperature estimation. *Geochem. Geophys. Geosyst.* **14**, 929–946.
- Toyofuku T., Kitazato H., Kawahata H., Tsuchiya M. and Nohara M. (2000) Evaluation of Mg/Ca thermometry in foraminifera: comparison of experimental results and measurements in nature. *Paleoceanography* **15**, 456–464.
- Toyofuku T., Matsuo M. Y., de Nooijer L. J., Nagai Y., Kawada S., Fujita K., Reichart G.-J., Nomaki H., Tsuchiya M., Sakaguchi H. and Kitazato H. (2017) Proton pumping accompanies calcification in foraminifera. *Nat. Commun.* **8**, 14145.
- Walsh J. J., McRoy C. P., Coachman L. K., Goering J. J., Nihoul J. J., Whitledge T. E., Blackburn T. H., Parker P. L., Wirick C. D., Shuert P. G., Grebmeier J. M., Springer A. M., Tripp R. D., Hansell D. A., Djenidi S., Deleersnijder E., Henriksen K., Lund B. A., Andersen P., Müller-Karger F. E. and Dean K. (1989) Carbon and nitrogen cycling within the Bering/Chukchi Seas: source regions for organic matter effecting AOU demands of the Arctic Ocean. *Prog. Oceanogr.* **22**, 277–359.
- Walton W. R. (1952) Techniques for recognition of living foraminifera. *Contrib. Cushman Found. Foraminifer. Res.* **3**, 56–60.
- Weldeab S., Arce A. and Kasten S. (2016) Mg/Ca- Δ CO₃ pore water-temperature calibration for Globobulimina spp.: a sensitive paleothermometer for deep-sea temperature reconstruction. *Earth Planet. Sci. Lett.* **438**, 95–102.
- Wollenburg J. (1992) Zur Taxonomie von rezenten benthischen Foraminiferen aus dem Nansen-Becken, Arktischer Ozean = Taxonomic notes on recent benthic Foraminifera from Nansen Basin, Arctic Ocean. 112, 137.
- Wollenburg J. (1995) Benthic foraminiferal assemblages in the Arctic Ocean: indicators for water mass distribution, productivity, and sea ice drift. Reports on Polar Research 179, 221.
- Wollenburg J. E. and Mackensen A. (1998a) Living benthic foraminifera from the central Arctic Ocean: faunal composition, standing stock and diversity. *Mar. Micropaleontol.* **34**, 153–185.
- Wollenburg J. E. and Mackensen A. (1998b) On the vertical distribution of living (Rose Bengal stained) benthic foraminifera in the Arctic Ocean. *J. Foraminifer. Res.* **28**, 268–285.
- Wollenburg J. E., Mackensen A. and Kuhnt W. (2007) Benthic foraminiferal biodiversity response to a changing Arctic palaeoclimate in the last 24,000 years. *Palaeogeogr. Palaeoclimatol. Palaeoecol.* **255**, 195–222.
- Woodgate R. A., Aagaard K. and Weingartner T. J. (2005) A year in the physical oceanography of the Chukchi Sea: moored measurements from autumn 1990–1991. *Deep Res. Part II Top. Stud. Oceanogr.* **52**, 3116–3149.
- Yu J. and Elderfield H. (2008) Mg/Ca in the benthic foraminifera *Cibicides wuellerstorfi* and *Cibicides mundulus*: temperature versus carbonate ion saturation. *Earth Planet. Sci. Lett.* **276**, 129–139.

Associate editor: Thomas M. Marchitto